

7292

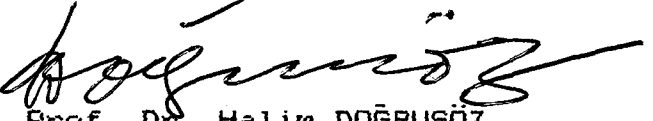
EFFECTS OF SOLUBLE BURNABLE POISON
ON THE AGE OF A PWR CORE

A MASTER'S THESIS
in
Nuclear Engineering
Middle East Technical University

T. C.
Yükseköğretim Kurulu
Dokümantasyon Merkezi


By
Serhat ALTEN
September 1987

Approval of the Graduate School of Natural and Applied Sciences


Prof. Dr. Halim DOĞRUSÖZ


Director

I certify that this thesis satisfies all requirements as a thesis for the degree of Master of Science in Nuclear Engineering Program of Mechanical Engineering Department.


Prof. Dr. Orhan YEŞİN

Chairman of the Department

We certify that we have read this thesis and that in our opinion it is fully adequate, in scope and quality, as a thesis for the degree of Master of Science in Nuclear Engineering Program of Mechanical Engineering Department.


Assoc. Prof. Dr. Güngör GÜNDÜZ

Supervisor

Examining committee in Charge:




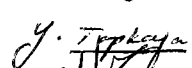

Prof. Dr. Namık Kemal ARAS (Chairman)

Assoc. Prof. Dr. Güngör GÜNDÜZ

Assoc. Prof. Dr. Tülay YEŞİN

Assoc. Prof. Dr. Yavuz TOPKAYA

Assoc. Prof. Dr. Mehmet KILDIR

ABSTRACT

EFFECTS OF SOLUBLE BURNABLE POISON
ON THE AGE OF A PWR CORE

ALTEN, Serhat

M.S. Thesis in Nuclear Engineering

Supervisor : Assoc. Prof. Dr. Gungor GUNDUZ

September 1987, 95 pages

The computer analysis of a PWR core to investigate the effect of soluble burnable poison on the age of fuel loading was studied. A multienergy, one dimensional, cylindrical geometry unit cell depletion code of LASER was used in the analysis.

It was found that, almost all core parameters could be improved by using soluble burnable poison due to hardening of neutron spectrum. Spectral hardening essentially results in more neutron capture in resonance region, thus more plutonium production, and consequently, increased core life.

Among eight different boration strategies studied, periodic boration followed by deboration toward the end of life, gives the highest power production per unit mass of spent U-235.

It was also found that 3.2 % fuel enrichment resulted in the best fuel economy for power production.



Key Words : PWR, Reactor control, Core age, Soluble poison, Boron.

ÖZET

ÇÖZÜNÜR VE YANAR ZEHİRLERİN PWR KALBİNİN ÖMRÜ ÜZERİNDEKİ ETKİLERİ

ALTEN, Serhat

Yüksek Lisans Tezi, Nükleer Mühendislik

Tez Yöneticisi : Doç. Dr. Güngör GÜNDÜZ

Eylül 1987, 95 sayfa

Bu çalışmada çözünür ve yanar zehirlerin PWR kalbine yüklenen yakıtın ömrü üzerindeki etkileri bilgisayarla incelenmiştir. Analizde, silindirik geometrili birim hacimde, çok enerji gruplu ve tek boyutlu yakıt tüketimi hesapları yapan LASER paket programı kullanılmıştır.

Reaktör kalbi ile ilgili bütün değişkenlerin, çözünür ve yanar zehirlerin kullanılması ile oluşan nötron dağılımının sertleşmesi nedeniyle geliştirilebildiği bulunmuştur. Spektrum sertleşmesi rezonans bölgesinde daha fazla nötron yutulmasına, daha fazla plutonyum üretilmesine ve kalp ömrünün artmasına neden olmaktadır.

İncelenen sekiz deęişik boron kullanım biçiminden birisi olan kesikli boron yükleme ve ömrün sonuna doğru boronu uzaklaştırma yöntemi, tüketilen birim yakıt için ençok enerji üretimini vermektedir.

Ayrıca, % 3.2 zenginleştirilmiş yakıtın güç üretimi açısından en uygun zenginleştirme olduğu bulunmuştur.



Anahtar Kelimeler : PWR, Reaktör kontrolü, Kalp ömrü, Çözünür zehirler, Boron

ACKNOWLEDGEMENT

The author would like to express his gratitude and greatest thanks to:

His supervisor, Assoc. Prof. Dr. Gungor GUNDUZ, for his kind patience, invaluable suggestions and helps throughout this investigation;

Prof. Dr. Orhan YESIN, for his encouragement and orientation during the entire period of his graduate study;

Officemates, and colleagues Ahmet OMURTAG, Ismail YAZICI, and Nihal CAKIR, for their advice, comments and suggestions;

Dr. Tuna BALKAN, for his kind help and guidance about the computer system;

Friend Ali Suat OZSOYLU, for his help and comments during the typing,

Friend Jale YIGIN, system responsible of CEKA Ins. Tic. A.S., for her hardware supply.

TABLE OF CONTENTS

	Pages
ABSTRACT	iii
OZET	v
ACKNOWLEDGEMENTS	vii
TABLE OF CONTENTS	viii
LIST OF TABLES	xi
LIST OF FIGURES	xii
NOMENCLATURE	xiv
1 INTRODUCTION	1
1.1 General	1
1.2 Scope of Present Study	4
2 REACTOR BURNUP PHYSICS	6
2.1 General	6
2.2 Fuel Management	8
2.2.1 Batch Loading	10
2.2.2 Zonal Loading	11
2.2.3 Scatter Loading	12
2.2.4 Axial Management	13
2.2.5 Recent Developments	13
2.3 Reactivity and Control Mechanisms	14
2.3.1 Movable Control Rods	19
2.3.2 Fixed Burnable Poison	21

2.3.3 Soluble Burnable Poison	24
2.3.4 Recent Developments	29
2.4 Fuel Depletion and Poison Accumulation	31
3 DEPLETION CALCULATION IN LASER	36
3.1 A Unit Cell Burnup Code LASER	36
3.1.1 Description of LASER	36
3.1.2 Control Aspects of LASER	39
3.1.3 Corrections and Additions	40
3.2 Input of LASER	41
3.2.1 Time Step Calculations	43
3.2.2 Specific Power Calculations	44
4 RESULTS	46
4.1 General	46
4.2 Results of Boration Strategy Search	47
4.3 Results of Enrichment Search	56
5 DISCUSSIONS	65
6 CONCLUSIONS	77
7 RECOMMENDATIONS	79
LIST OF REFERENCES	81
APPENDICES	83
A. Nuclear Power Capacity Projections	83
B. Control Layout of LASER	84
C. Files of LASER	86
D. Changes in LASER	87

E. Some Basic Equations	90
F. Determination of Xenon and Samarium Time Steps	92
G. Solution of First Order Differential Equation	94



LIST OF TABLES

Table	Pages
2.1 Comparison of neutronic features of control methods	29
3.1 Sample PWR data	41
3.2 Input of LASER for sample PWR	42
3.3 Isotopic composition of UO ₂ fuel for different enrichments	42
4.1 Boron concentrations in ppm	49
4.2 Specific power calculations	55
4.3 Some isotopic accumulated results at EOL	56
4.4 Boron concentrations in each time step of BD case in ppm units	57
4.5 EOL results of 2.1 % enrichment	57
4.6 EOL results of 4.0 % enrichment	57
4.7 EOL results of 4.8 % enrichment	60
4.8 EOL results of 5.6 % enrichment	62
4.9 Specific power calculations of cases BD at different enrichments	62
5.1 Case evaluation for various criteria	73
A.1 Nuclear power production	83
C.1 File descriptions that are used in LASER	85

LIST OF FIGURES

Fig.	Pages
2.1 General behaviour of radial change of thermal flux (ϕ)	9
2.2 Simple sketch of three-batch zonal loading ...	11
2.3 In-out scatter loading	12
2.4 Cluster control assembly for PWRs	20
2.5 Comparison of depletion characteristics of gadolinium and boron	23
2.6 A model of coolant and boron control system ..	25
2.7 Power distribution in three-zone core a) using rod control, b) using chemical shim control	26
2.8 Change of moderator temperature coefficient with moderator temperature at different boron concentration	28
2.9 Effects of different poisons on critical lattice	30
2.10 Fuel depletion chain for uranium fueled reactor	31
2.11 Production and removal of Xe-135 in fission ..	33
2.12 Production and removal of Sm-149 in fission ..	33

3.1	Unit cell of LASER for square batch	38
4.1	Change of k_{eff} and required criticality boron concentration for 3.2 % enrichments	48
4.2	Cell averaged thermal flux	49
4.3	Cell averaged fast flux	50
4.4	Cell averaged epithermal flux	51
4.5	Radial thermal flux distribution for different initial boration values at the initial time step	52
4.6	Xenon transients at early stages of core life	53
4.7	Changes of k_{eff} at different boration strategies for 3.2 % enrichment	54
4.8	Depletion characteristics of boron in case CB	55
4.9	Changes of k_{eff} at different enrichments for NB case	58
4.10	Criticality boron concentrations for CB case .	59
4.11	Change of k_{eff} for 2.1 % enrichment	60
4.12	Change of k_{eff} for 4.0 % enrichment	60
4.13	Change of k_{eff} for 4.8 % enrichment	61
4.14	Change of k_{eff} for 5.6 % enrichment	61
4.15	Cell averaged thermal flux change at various enrichments for BD case	63
4.16	Fission product poisoning at EDL	64
4.17	Change of specific power	64
B.1	General flowchart of LASER main program	85
D.1	Boron depletion calculations added to LASER ..	87

NOMENCLATURE

Symbols

a, b, c, d	arbitrary constants
A	atomic weight (amu)
B	buckling (cm ²)
E _t	total energy produced at EOL (GWD)
E _{xx}	^{xx} *10
f	fuel utilization factor
H	active height of core (cm)
I	atom density of iodine (atom/cm ³)
k	multiplication factor
M	mass (kg)
N	atom density (atom/cm ³)
N ₀	Avagadro's number
n	neutron
p	resonance escape probability
P	nonleakage probability
P _t	thermal nonleakage probability
P _{sp}	specific power (GWD/kg)
P	atom density of promethium (atom/cm ³)
R	equivalent active radius of core (cm)
r	radius (cm)

S	atom density of samarium (atom/cm ³)
T	temperature (K)
t	thickness (cm)
t	time (s)
v	void coefficient of moderator
X	atom density of xenon (atom/cm ³)
α	reactivity coefficient
Γ	fission yield
λ	decay constant (s ⁻¹)
μ	reactivity
μ	density (gr/cm ³)
Σ	macroscopic cross section (cm ⁻¹)
σ	microscopic cross section (cm ²)
τ	core age (GWD/T)
ϕ	neutron flux (n/cm ² s)
ϵ	fast fission factor
η	# of neutrons appears as a result of fission by absorption of one neutron

Subscripts

a	absorption
ass	assembly
b	boron
eqm	equilibrium
eff	effective
f	fission
i	iodine
p	promethium
s	samarium
x	xenon

CHAPTER 1

INTRODUCTION

1.1 GENERAL

The world's first fossil fueled electric power plant went into operation at 750 kW capacity in New York city in 1882. In the 20th century, a new source of energy was born, the Nuclear Energy. After the discovery of neutron by Chadwick in 1932, experiments on neutron bombardment of heavy atoms were performed. Three scientists, Leo Szilard, Enrico Fermi, and Otto Hahn, independently did very valuable work at about the same time. Although Leo Szilard patented the "Chain Reaction" in 1934, first reactor was built up by Enrico Fermi at the University of Chicago. It was a graphite moderated reactor, and reached the criticality in 1942. The purpose of Fermi reactor was not the power production but the production of plutonium for atomic bomb.

After the 2nd World War, the world's first nuclear power plant was put into operation in 1954 in USSR. Nuclear technology advanced quickly in the last few decades to meet the world's energy demand of the world as it is the most comprehensive energy source after the

fossil fuels. In the first two decades of nuclear era, Pressurized Water Reactors (PWR), Boiling Water Reactors (BWR), Gas Cooled Thermal Reactors (GCTR), and Heavy Water Reactors (HWR) were the main reactor types for production of steam from nuclear energy. PWR and BWR use enriched uranium while the other two use natural uranium for fuel.

Since the sources of uranium are limited, the nuclear power industry is being planned out to shift to the breeder reactors in the coming decades. Breeding is defined as the production of fissile isotopes from non-fissile fuel isotopes, e.g. Pu-239 production from U-238 (See Fig. 2.11). The main types of breeder reactors that are under-development, are Liquid Metal Fast Breeder Reactors (LMFBR), Gas Cooled Fast breeder Reactors (GCFR), and Molten Salt Breeder Reactors (MSBR).

With the advance of the nuclear technology, nuclear power became the primary energy source in a number of countries like France, Taiwan, Belgium, and Sweden [19]. Today's capacity of nuclear power plants and capacity projections for the year of 1990 and 2000 for various countries were given in App. A. It can be seen from Table A.1 that, the nuclear energy is an important alternative to fossil fuels, not only for developed countries but also for developing countries. Although the types of reactors were not mentioned in this table, PWR is the most commonly used reactor all over the world.

Early nuclear reactors were controlled by using strong neutron absorbers. Such control rods were said to be "black". Strong flux depressions at certain locations of reactors caused unsmooth power production, and inefficient burning of fuel, while thermal stresses introduced early material failure problems. So, recent control rods are made from relatively weak neutron absorbers and these rods are said to be "gray".

Around 1964, a new control aspect so-called soluble burnable poison control was developed for PWRs. Strong neutron absorbers such as cadmium, indium, and boron are injected into the primary coolant system from the high concentration tanks (See Fig. 2.6) for absorbing the excess reactivity, defined as " $k-1$ ", of the core. Owing to the sensitivity of the amount of soluble poison in the core to the coolant/moderator density, soluble poison control is a technology mainly for PWRs. However, some researchs are carried out to use it also in other reactor types. By using soluble poison, the volume of control rods for absorbing the excess reactivity can be decreased due to spectral hardening.

1.2 SCOPE OF PRESENT STUDY

The primary source of the economic advantages of nuclear power over the conventional power sources lies in the substantially lower fuel costs of nuclear power reactors. Therefore, an extremely important facet of nuclear engineering involves determining the parameters of both, the initial core as well as the subsequent reload cores to minimize fuel costs. This topic is known as in-core fuel management, and extending the core life of the reactor is the primary aim of the current studies.

Core life or cycle length can be defined as the time during which the core can be kept critical for each loading. If the loaded fuel is enriched, it is obvious that the core life will increase, but the economy gained may not always be of high significance. Fuel enrichment is an expensive process which leads to an increase in fuel costs. In addition, with the increase in enrichment, initial multiplication factor of core will increase. This then increases the control requirements of the core. In other words, more volume is needed for absorbing excess neutrons.

The aim of this research is to find the optimum amount of soluble burnable poison for a given enrichment. The optimum soluble burnable poison denotes the amount which gives the maximum core age and the maximum power

production per unit mass of spent fuel. The change in some reactor parameters, such as U-235 depletion, Pu-239 production, isotopic power production rates, etc. were also given.

A sample PWR core data was used in the execution of unit cell depletion code, LASER [1,18] which will be described later in Chapter 3. The enrichment of the fuel loading was changed from 2.1 % to 5.6 %.

The present study includes a brief description of in-core fuel management, control methods and fuel depletion in Chapter 2. Chapter 3 consists of some introduction about LASER code used and its data. In Chapter 4, the results of the study were given. Discussion of results, conclusions, and recommendations, were presented in Chapters 5,6, and 7, respectively.

CHAPTER 2

REACTOR BURNUP PHYSICS

2.1 GENERAL

Nuclear analysis of a reactor core can be divided into three as core criticality and power distribution, reactivity and control, and depletion analysis [3]. All three analysis require an accurate burnup prediction.

The most accurate fuel burnup data can be obtained by experimental, destructive or non-destructive methods. In the destructive method, the irradiated fuel element is analyzed by radiochemical techniques to find the overall burnup of fuel. The non-destructive method consists of the gamma ray analysis of irradiated fuel [5]. But, in the design steps of a nuclear reactor, a burnup prediction is required to get a knowledge about the future behaviour of core, therefore, burnup calculations must be carried out by using simulation computer programs.

Reactor core behaviour can be predicted by criticality calculations over the core life while flux distribution calculations are mainly used to determine the loading pattern of fuel. Both criticality and flux

distribution are dependent on the depletion of fuel.

The excess reactivity of fuel loading must be known in design steps, to achieve the best control strategy and the fuel loading pattern for flexible and safe operation of a reactor. The fuel composition change during the core life and the fission product accumulation with the depletion of fuel must also be known by the designer for the above goals.

In other words, a complete study of the time dependent production and depletion of nuclei in the core which is called as depletion or burnup analysis, must be performed in the design stages. The burnup analysis of a reactor core is used in the determination of main problems of core design, control mechanisms, fuel management, and consequently, core age. The last one is the most important parameter used in design in which the optimization problems are done for the better burnup of fuel. The better burnup naturally means higher core age.

Core age (τ) is defined by the units of power produced in total life of core per unit mass of fuel loaded (MWD/T) or in units of effective number of days in which the reactor has been operated at 100 % full power output (EFPD). Some other units can also be introduced as power produced during the core life per unit mass of spent fuel (P_{sp} = Specific power) which is used in this study as a comparison criterion.

In power reactors, core age in MWD/T depends upon some parameters, as initial fuel load and enrichment, zoning, burnable poison utilization, predicted conversion ratio, etc.. If the different amount of utilization of control mechanisms is called as "control strategy", the relationship between this strategy and core age is a remarkable question. For a better approach, some more details about the fuel management and the control mechanisms need to be introduced.

2.2. FUEL MANAGEMENT

In a nuclear reactor core, radial flux distribution (or power distribution) shows a similar behaviour to "arbitrary flux" in Fig. 2.1 without the control elements. The area under the curve is proportional to the total power generation, therefore the greater the area under the curve, the more the power generation in the reactor. But, there are some constraints about the flux distribution. The maximum flux can not exceed a certain value because the local temperature increases with the power generated and with the local flux present. Then, the area can not be arbitrarily improved by increasing the flux, if the design value of the flux is close to the limiting value. On the other hand, flux can be flattened by using different loading patterns and/or proper utilization of some control

mechanisms. The most important loading patterns used in practice are batch loading, zonal loading, and scatter loading. By flux flattening, some power can be gained, i.e

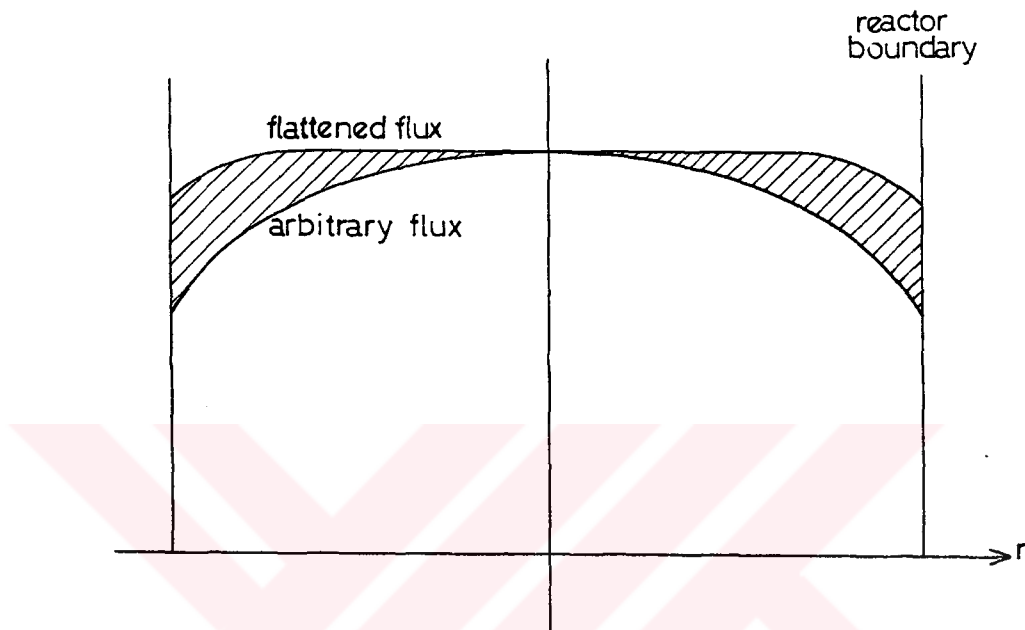


Figure 2.1 General behaviour of radial change of thermal flux (ϕ)

area under the curve can be increased. The area which can be gained lies between the arbitrary flux curve and the flattened flux curve, that is the shaded area given in Fig. 2.1. Flux flattening is a fundamental issue in fuel management.

A fuel manager has the flexibility of using some variables when choosing the reload patterns mentioned earlier. These variables are [4];

1. enrichment of fresh fuel,

2. quantity of fresh fuel (number of new fuel elements),
3. reuse of used fuel.
4. length of a reactor fuel cycle, i.e the residence time of each fuel batch in the reactor,
5. detailed reloading pattern,
6. altering the mechanical design of the fuel assembly,
7. use of burnable poisons.

The last one will be discussed in detail later. The criteria used in optimizing in-core fuel management schemes can be summarized as [4];

1. maximizing average discharge fuel burnup,
2. maximizing cycle length (or k_{eff} , or cycle burnup),
3. minimizing fresh reload fuel (or enrichment),
4. minimizing power peaking factor (or maximizing core power).

2.2.1 Batch Loading

The oldest method of reactor core fuel loading is the batch type in which all the fuel elements has the same enrichment in the reactor core. At the end of cycle (EOC), all fuel elements are replaced with the fresh ones, and this is repeated for each cycle. Batch type, or so-called single batch type loading has a great disadvantage, radial flux or power distribution cannot be controlled by loading.

2.2.2 Zonal Loading

This type of loading is the first modified case of batch loading which is also called as the In-Out cycling. In order to have flattened flux distribution or more power, a multi-zoned fuel loading pattern (Fig. 2.2) is applied in which the enrichment of each zone decreases through the inner zones at the initial cycle. If the batch

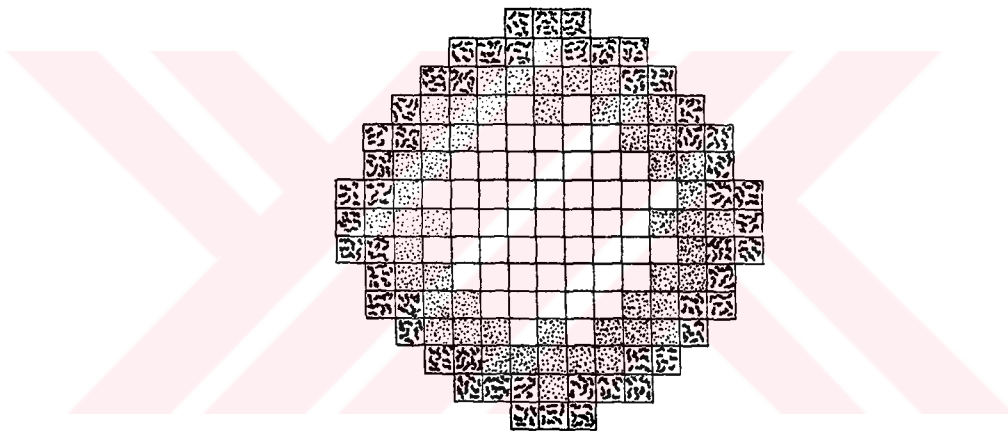


Figure 2.2 Simple sketch of three-batch zonal loading

is defined as the certain fraction of core replaced during each refuelling, then zones correspond to single batches. Irradiated (or partially used) batches are shifted towards the inner zones while the central zone is withdrawn from the core and fresh fuel is charged to the outermost zone. The fresh fuel at the outermost zone causes a strong flux gradient at the core boundary, enhancing the neutron leakage. Irradiated fuel at the center of the core avoids

high power peaking. In large cores subjected to high burnups, appreciable distortions in the flux distribution can arise which could lead to large power peaking factors.

2.2.3 Scatter Loading

The disadvantage of zonal loading, i.e. rather high power peaking factors had led a new pattern. In order to exploit the local and global flux flattening simultaneously, fuel is loaded in a scatter, or random pattern. In the modified in-out scatter loading (Fig. 2.3), the fresh fuel is charged as first batch to the edge of the core while the irradiated fuel in the outer zone is scatter loaded in the inner zones. After the first few transient cycles due to mainly fission product poisoning, core reaches to equilibrium with equal power production in

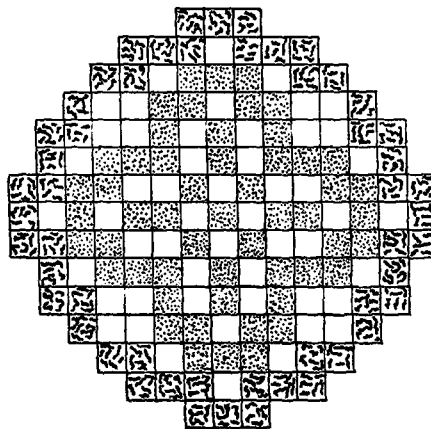


Figure 2.3 In-Out scatter loading

each cycle. Therefore, the radial power distribution which is characterizing a scatter-loaded core, has a somewhat flattened form of the distribution characterizing a single batch loading core. However, there are very small distortions in the local power density. Three-batch in-out scatter loadings are frequently used in PWRs while BWRs employ usually four-batch scheme [6].

2.2.4 Axial Management

Design specifications of fuel allow to radial power shaping in the reactor but a similar flux distribution is valid in axial direction. An alternative of axial flux shaping is the change in fuel composition of fuel element axially. But for the reason of added fabrication costs, PWR's or BWR's fuel rods are uniform in axial direction.

The axial fuel management is handled by control mechanisms which will be discussed later, and by coolant management rather than axial enrichment zones. Varying the coolant flow rate affects the heat transfer to the coolant, and consequently, the fuel temperature. The Doppler feedback couples on the corresponding reactivity change [6].

2.2.5 Recent Developments

Recent developments on fuel management are based on the out-in scattering loading pattern mainly. Method is

improved by using different enrichment loading pattern in also successive cycles. Downar and Kim performed such a pattern for optimizing the beginning of cycle (BOC) power at Zion Unit 1 PWR [7]. Loading pattern of Zion Unit 1 consists of four different enrichment in each cycle which means each batch has differently enriched fuel assemblies.

Hobson and Turinsky [8], approached to the problem with a new method. Their optimization model was based on an additional classification of fuel elements, called "color". Each color fuel assembly has different burnup with different reactivity. The color assignment scheme was based on fuel assembly reactivity ranking, with color 1 being associated with the lowest reactivity fuel assembly. A kind of out-in scattering loading pattern has been used by considering the colors, for maximizing BOC cycle reactivity within power peaking and burnup constraints in LEOPARD and PDD codes.

Economic analysis of advanced in-core fuel management techniques can be seen in the study of Andrews, Matzie and Shapiro [9].

2.3 REACTIVITY AND CONTROL MECHANISMS

Criticality of the reactor is described by the condition of " $k=1$ " and disturbances in the core is expressed by the deviation from the unity. The relative

deviation,

$$\mu = \frac{k-1}{k}$$

2.1

is known as the reactivity of the core where k is the multiplication factor. Excess reactivity is compensated by control mechanisms. Balancing of reactivity components which cause negative or positive change, continue until zero excess reactivity, i.e core life. Here, the excess reactivity is defined as the case, all the control systems are withdrawn from the core.

The main component of reactivity is due to fuel which introduces positive reactivity. A certain amount of negative reactivity, control reactivity must be introduced into the core for compensating the excess reactivity of the fuel. There are also some other control reactivities for proper control of the core. These can be classified as; i) scram control for shutting the reactor down under any conditions which requires very rapid negative reactivity insertion, ii) power regulation designed to cover the small reactivity transients due to changes in reactor parameters, and iii) shim control for compensating long term reactivity changes due to fuel depletion, and fission product buildup.

So, essentially two main reactivity changes can be described as long term and short term reactivity deviations. The causes of long term reactivity changes are

the fuel depletion and the fission product poisoning, and they adversely affect each other. Since the core is loaded with a fuel more than the critical mass, a certain amount of positive reactivity is already inserted into the core. By fuel depletion, the reactivity of the system increases with the appearance of about 2.4 neutrons in fission process with the absorption of single neutron. Inversely, fuel depletion introduces negative reactivity due to fission product accumulation. Each fission product has a certain absorption cross section but two of them, xenon-135 and samarium-149 have very large cross sections. Excess neutron absorption by Xe-135 and Sm-149 is known as fission product poisoning and it has a negative effect on the reactivity. It must be noted that, they are depleted by neutron absorption, while Xe-135 additionally undergoes radioactive decay, so, both reach equilibrium in time. Therefore, time dependent effect of fission product poisoning must be considered in early times of operation only.

The short term reactivity changes are usually due to spontaneous events. Rapid changes of some operational parameters of core cause changes in reactivity. The temperature of fuel and of moderator are highly sensitive to flux changes. Sudden changes in flux, i.e power peakings result in change of temperature which affects the fission rate of fuel directly. Therefore, negative effects of temperature on the reactivity must be achieved for the

safe operation of power reactors. The change of reactivity with the temperature is given by formula;

$$\alpha_T = \frac{1}{k} \frac{dk}{dT} \quad 2.2$$

where α_T is the temperature coefficient of reactivity, and T is the temperature. Eqn. 2.2 is applicable for both fuel and moderator.

The response of a reactor to a change in temperature, depends on the sign of the coefficient of reactivity. If α_T is positive, an increase in temperature results in an increase in k . It then increases the power which in turn, results in an increase in temperature again. This leads another increase in k and so on. Therefore, any increase in temperature will lead to the melt-down of the core in the absence of external intervention. Similarly, a decrease in temperature will result in shut-down of the reactor. If α_T is negative, the process is entirely different. Any change in temperature will result an inverse effect on power by an opposite change in k , and that forces the temperature to return to its original state. For instance, if the temperature of the moderator increases, thermalization rate drops, so fission decreases and power decreases, then temperature decreases and thermalization rate increase to restore the original state.

The fuel temperature coefficient of reactivity is negative for all reactors owing to a phenomenon known as nuclear Doppler effect [2]. The moderator temperature coefficient can be approximately written based on the six factor formula as,

$$\alpha_{T, mod} = \alpha_{T, f} + \alpha_{T, p} + \alpha_{T, P} \quad 2.3$$

where f is the fuel utilization factor, p is the resonance escape probability, and P is the nonleakage probability. These are the temperature dependent properties of well known equation,

$$k = \eta \epsilon f p P_t \quad 2.4$$

and each term of Eon 2.3 is defined as given by Eon. 2.2, for instance for f ,

$$\alpha_{T, f} = \frac{1}{f} \frac{df}{dT} \quad 2.5$$

$\alpha_{T, f}$ depends on temperature due to the expulsion of some of the liquid moderator from the core with increasing temperature. The reduced absorption of moderator relative to absorption of fuel, results in an increase in f , therefore, α_T will be positive. This effect is especially important in the case when the soluble poison is present in the moderator. Ejection of some moderator due to an increase in temperature leads to a decrease in p which results in a negative α_T for a liquid moderator. Same phenomenon results in a decrease in P in a more complex manner, and causes negative α_T . This is simply due to the fact that neutrons diffuse more readily through less dense media, and leakage of neutrons increases with

increasing temperature.

There are some other coefficients, such as void coefficient of reactivity,

$$\alpha_v = \frac{d\alpha}{dv} \quad 2.6$$

for void coefficient of moderator v , and it is highly important in BWRs. Besides these inherent reactivity changes, some different methods of negative reactivity insertion are used for different control requirements, mainly for balancing positive reactivity, such as control rods, fixed burnable poisons, and soluble burnable poisons, i.e. chemical shim.

2.3.1 Movable Control Rods

Control rods are used for many purposes, power regulation, scram control, and partly in shim control. Cluster type control rods (Fig. 2.4) are mainly used in PWRs [3]. Absorber rods used in PWRs compose of hafnium (or indium), cadmium and silver generally, and they absorb neutrons from thermal and intermittent energy ranges. With the increase in control requirement in which the control rods are used, the total volume occupied by them increases, and it leads to an increase in overall size of core.

For scram, rods must have high amount of negative reactivity for shutting the reactor down in emergency case. Control rods have the most reliability for this purpose, especially due to mechanical availability of required speed of reactivity insertion.

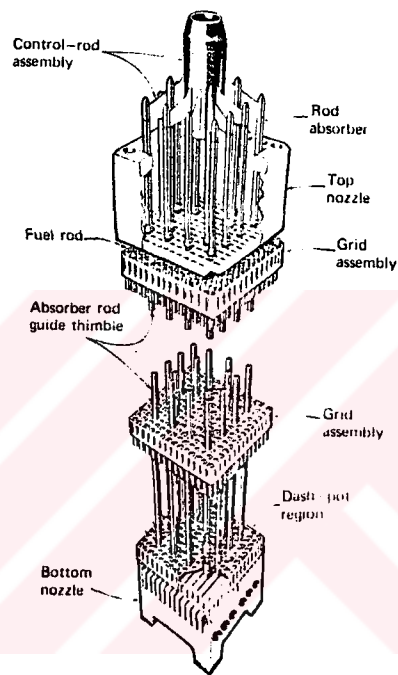


Figure 2.4 Cluster control assembly for PWRs

Xenon and samarium transients are also controlled by control rods. When the fission increases after the start up, fission products accumulate in the time and they introduce a negative reactivity to the system. This is compensated by the withdrawal of control rods from the core. Since the reactor started up with all rods fully inserted into the core, a positive reactivity is inserted into the system by withdrawal. The positive reactivity is

balanced by the accumulation of Xe-135 and Sm-149.

The small transients in the reactivity are controlled by the partial use of control rods. The hot spots in the cell are also removed by the partial insertion of rods.

Fuel management using control methods is an important subject in which no modification of reactor core design is necessary. By using control rods, flux distribution can be controlled with a loss in neutron economy. Flux flattening can be obtained with a proper utilization of all rods, but too much neutrons must be absorbed which is undesirable. Additionally, axial distribution of flux cannot be controlled with full length control rods. Therefore, control rods containing neutron absorbers only at a certain portion so-called Axial Power Shaping Rods (APSR) can be used. A fuel management study by using APSRs had been performed for Rancho Seco core by Ake et al. [10]. They tried to develop a new procedure of APSR withdrawal for extending the fuel cycle length.

2.3.2 Fixed Burnable Poison

A relatively new concept in the control of a reactor is the use of fixed burnable poisons for long term reactivity changes and it is the most suitable control method for fuel management. Burnable poison pins are placed in an assembly like the absorber rods shown in Fig. 2.4. Burnable poisons are such isotopes that they have

high absorption cross sections and are converted into nuclides with low absorption cross sections after the neutron absorption. The mostly used element is boron and there is a high tendency for the use of gadolinium also. Burnable poisons can be placed uniformly mixed with the fuel. In this respect, gadolinium oxide draw more attention than boron because it is more compatible than boron carbide. Since they have higher cross section than the fuel, they burn out more rapidly leaving minimal poison residue at the end of cycle. For boron based burnable poisons, residual poison can be in significant amount, and since it is fixed mechanically, there is no way to withdraw it.

Radial power distribution control is easily achievable with proper location of the burnable poison. So, preloading determination of the poison control design is required where flexibility in placing different poison pins within one assembly provides an additional degree of freedom in the design. The optimization of reloading of the nuclear reactors depends completely on the successful utilization of burnable poisons to provide the required depletion or power distribution [11].

As mentioned earlier, gadolinium can deplete at a much greater rate due to much higher thermal absorption cross section, resulting in minimum residual poison. A comparison of burning rates of these two materials were

17x17 assembly type

	Poison	Poison pin/assem.	Initial poison concentration
1B	B4C/A1203	24	3.2 wt% boron natural
2B	B4C/A1203	20	5.6
3B	B4C/A1203	16	12.5
1G	Gd2O3/UO2	24	3.1 wt% Gd2O3
2G	Gd2O3/UO2	20	4.6
3G	Gd2O3/UO2	16	8.6

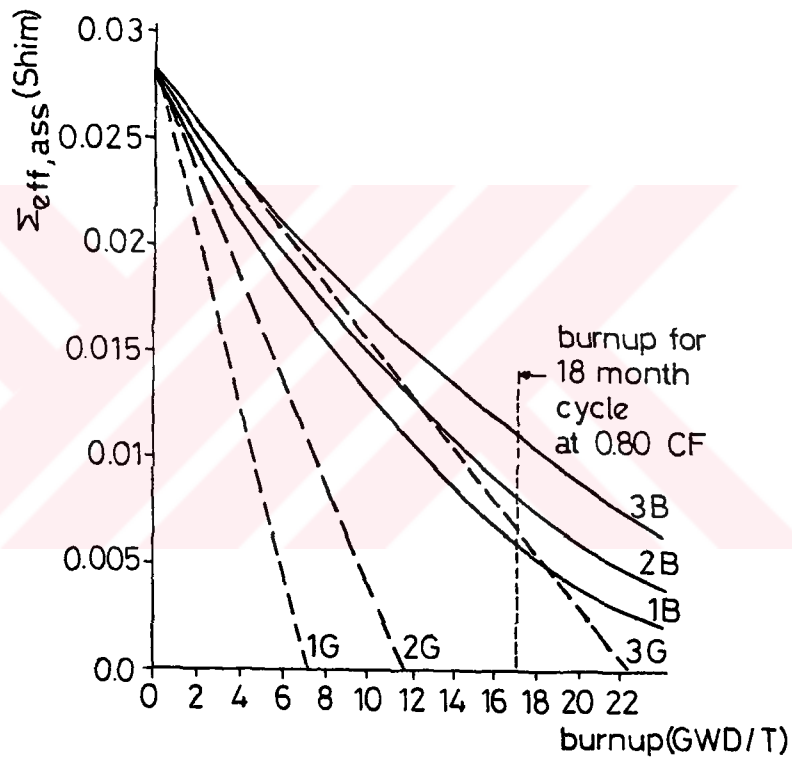


Figure 2.5 Comparison of depletion characteristics of gadolinium and boron

shown in Fig. 2.5 [12]. It is seen that, significant amount of EOC residual poison still remains in the case of boron even in the minimum boron concentration (i.e 1B in Fig. 2.5). For gadolinium, an important characteristics can be seen from the Fig. 2.5 that the slopes of curves

largely depend on the initial concentration, i.e. the number of poison rods per assembly. In addition, no residual poison remains in two of the three cases in this study, only one of them exceeds cycle length.

Power distribution can be significantly improved by burnable poisons for two reasons [13]; i) control rods, except those required for xenon and samarium transient, can be removed from the core during operation which reduces the flux distortion, and ii) a further improvement can be obtained by locating the burnable poison where the flux tends to peak, which reduces the peaks and leads to a uniform power distribution throughout the core.

The last important property of burnable poisons that must be pointed, is the tendency of burnable poisons to make the reactivity temperature coefficient of core more negative, which results in increased safety, stability and self-regulation of core. The general tendency in the design of new PWRs is to use only burnable poisons for steady operation, and to use control rods for abrupt reactivity changes.

2.3.3 Soluble Burnable Poison

Soluble poison or chemical shim is a kind of control based on a material having high neutron absorption cross section with solubility property in the moderator. Boric

acid is used in most of the applications in ppm (parts per million) units in the moderator. Soluble poisons are used for long term reactivity changes, and permits a reactor to be operated at full power, in the steady state condition with all control rods in the "out" position except for the small transient controls. Therefore, a saving of more than 50 % in the number of control rods, drive mechanism and associated equipment is possible [13]. But injection and removal of the boric acid into and out from the moderator also require a complex scheme that can be seen in Fig. 2.6 [14]. But this complex scheme and poisoning takes place away from the fuel region, i.e. there is no relation with

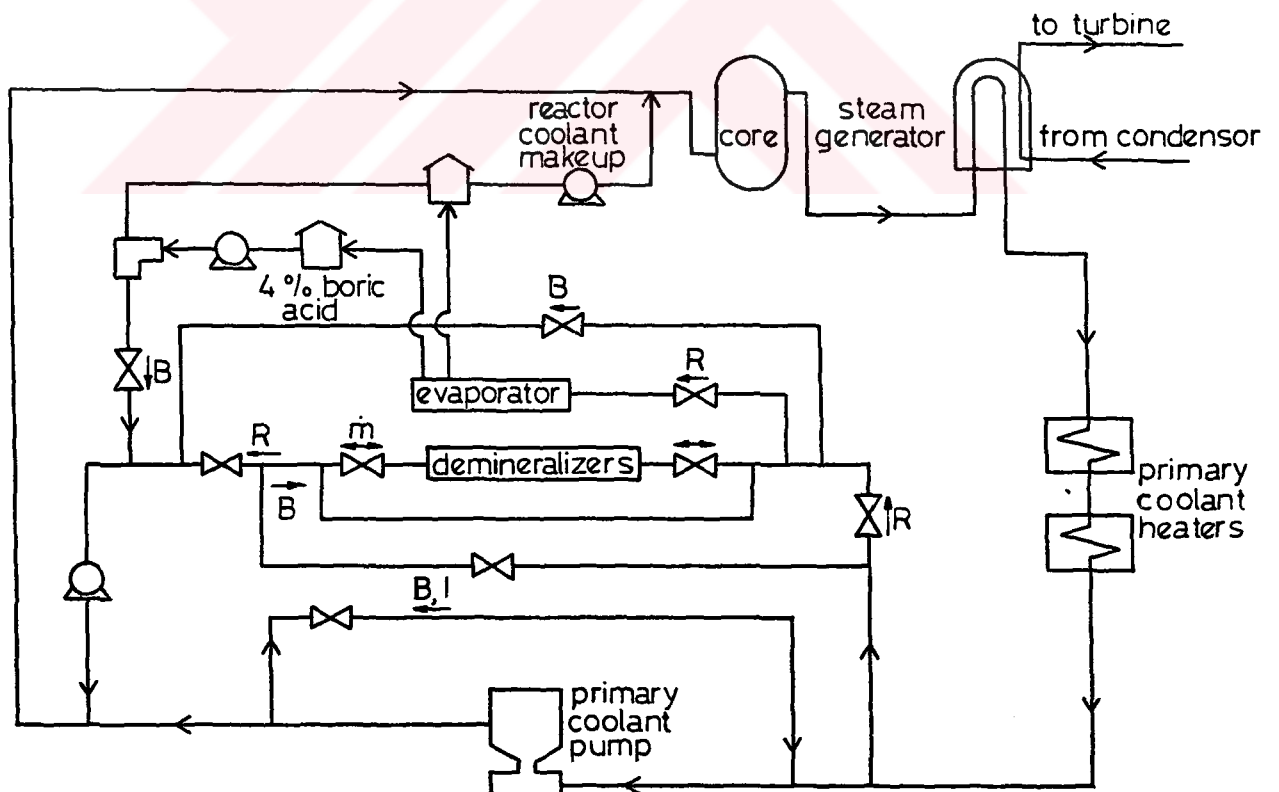


Figure 2.6 A model of coolant and boron control system (B=boration, R=removal, I=inactive)

the fuel volume. This is another reason why it is preferably used. Both control rods and fixed burnable poisons are in such positions which can also be used for fuels. In other words, some of the fuel element tubes are substituted by control rod tubes, and fixed burnable poison tubes in a reactor. But, the lessened need for the control rods because of the addition of soluble poison provides the possibility of inserting more fuel elements into the core. Hence, the core age can be further increased.

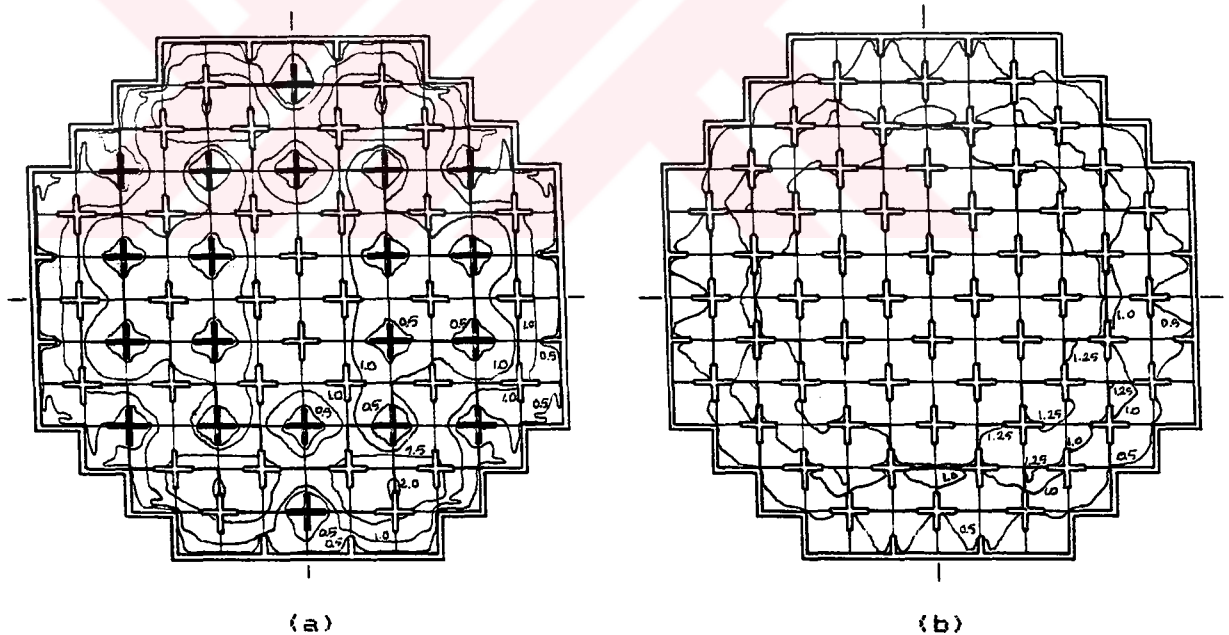


Figure 2.7 Power distribution in three-zone core, a) using rod control, b) using chemical shim control

Since the soluble poison is injected into the moderator uniformly, radial flux distribution is not flattened but suppressed, therefore, fuel loading pattern does not essentially change compared to non-poison case. Soluble poison utilization does not introduce complexity into the calculations of fuel management. A comparison of flux distribution of control rod and soluble poison utilization in a three batch loading can be seen in Fig. 2.7 [13]. Control rods, shown by crosses in Fig. 2.7.a, disturb the power distribution more than the soluble poison does as seen in Fig. 2.7.b.

The temperature coefficient of moderator with soluble poison becomes less negative compared to non-poison case, because higher reduction in absorption of moderator occurs with the expulsion of liquid by increase in temperature. This naturally means higher positive $\alpha_{T,f}$ and/or less negative α_T . In addition, chemical poison density decreases with an increase in temperature, and this gives rise to positive component of reactivity which is directly proportional to poison concentration [13]. Neutron absorption by control rods contributes a negative increment to the coefficient. But, since the soluble poison is used in controlling the excess reactivity with control rods almost withdrawn, the initial temperature coefficient of reactivity becomes less negative as burnup increases. After a certain burnup, i.e. certain poison

concentration, it will be positive, especially at low temperatures as seen from Fig. 2.8. It had been found that, with a zero or even positive temperature reactivity coefficient, core stability is not adversely affected if the net coefficient (poison independent Doppler and moderator) remains only slightly positive [13]. Consequently, to keep the α_T negative, initial concentration of poison loaded must not exceed a certain value for certain loading.

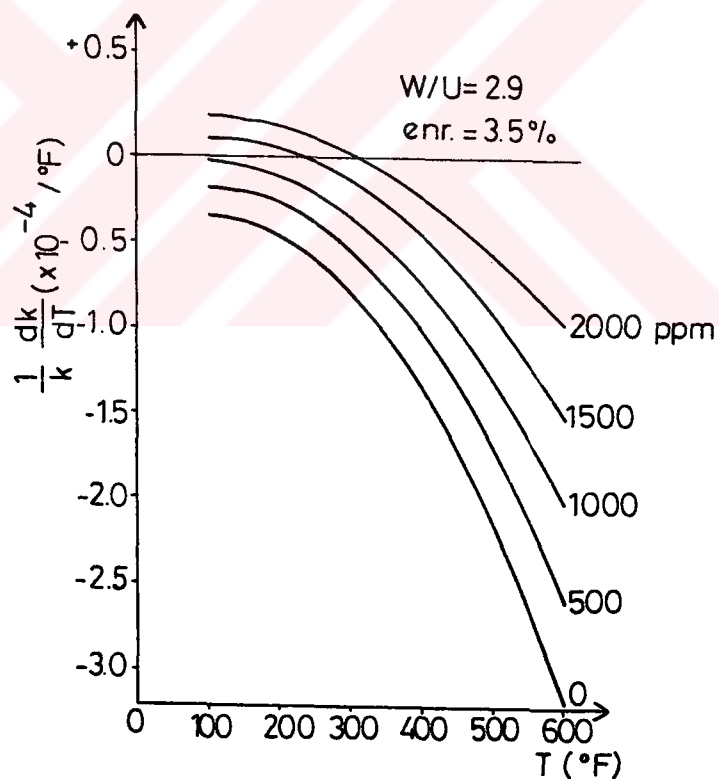


Figure 2.8 Change of moderator temperature coefficient with moderator temperature at different boron concentration

Finally, another limitation for boron utilization is the rate of boron injection and/or withdrawal into and out from the system due to mechanical constraints. Maximum reactivity injection rate is about $3.0 \text{ E-}05 \text{ s}^{-1}$ [3]. Hence, soluble poison can be used for only long term reactivity changes.

2.3.4 Recent Developments

Ronen and Galperin suggested a new PWR control system in which gaseous absorber is used [15]. This method is based on the introduction of a neutron absorber gas, He-3, which has a very high absorption cross section, into the reactor core. They proposed to inject the absorber gas into the guide timbles which can be connected to tubes, so that the pressure of the gas in these timbles may be controlled. A comparison of three control methods and the suggested one is tabulated in Table 2.1 [15].

Table 2.1 Comparison of neutronic features of control methods

method of control	scram contr.	void coef.	axial power distr.	power regul.	radial power distr. contr.	unneces sary neutron absorp.
Control rods	Yes	No	Yes	Yes	Yes	No
Burnable poison	No	No	No	No	Yes	Yes
Soluble poison	No	Yes	No	Yes	No	No
Poisonous gas	Yes	No	No	Yes	No	No

Galperin et al. [16] proposed the substitution of soluble poison reactivity control system of a PWR by gadolinium as a fixed burnable poison. Usually, only the first core is loaded with fixed burnable poisons, while in the equilibrium cycles, only the soluble poison and generally boron is used to control the core criticality.

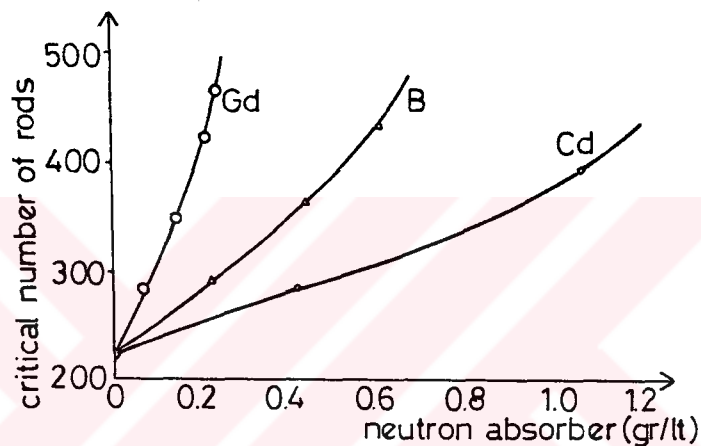


Figure 2.9 Effects of different poisons on critical lattice

While the traditional element of soluble poison is boron, Lloyd et al. [17] proposed the utilization of gadolinium and cadmium as soluble poisons. A series of experiments had been performed to compare the effects of poisons on the criticality of water moderated lattice assembly. Their results can be seen in Fig. 2.9.

2.4 FUEL DEPLETION AND POISON ACCUMULATION

During the operation, the fuel composition will change as fissile isotopes are consumed and fission products are produced. Core life analysis requires studying the time dependent depletion and production chains for principal isotopes. In fuel depletion point of view, main isotopes are uranium and plutonium isotopes, and their depletion chains can be seen in Fig. 2.10.

Fuel depletion analysis is concerned with predicting the long term reactivity changes. Therefore, a detailed analysis of time dependent fuel depletion analysis is required for defining the core life of a reactor and its control.

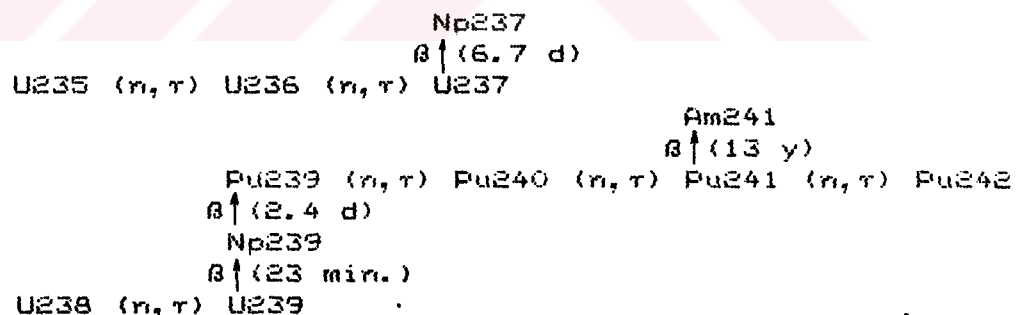


Figure 2.10 Fuel depletion chain for uranium fueled reactor

Since the fission is almost always asymmetric, two fragments have different masses, and each fragment appears with a certain fission yield which is given as a function

of mass number in literature [2,3]. In this wide spectrum of fragments, i.e between the mass numbers of 70 to 160, two of them, Xe-135 and Sm-149 are important due to their high absorption cross sections. The thermal neutron absorption cross sections are 41000 barns for Sm-149 and 2.7×10^6 barns for Xe-135 [2].

Production and removal of Xe-135 can be seen in Fig. 2.11. But, half lives of some of the precursors of Xe-135 are so small, therefore, Xe-135 concentration at any time t can be expressed by considering the iodine only as follows;

$$\frac{\delta I}{\delta t} = \Gamma_1 \Sigma_f \phi(r,t) - \lambda_1 I(r,t) \quad 2.7$$

$$\frac{\delta X}{\delta t} = \Gamma_x \Sigma_f \phi(r,t) + \lambda_1 I(r,t) - \lambda_x X(r,t) - \sigma_{a,x} \phi(r,t) X(r,t) \quad 2.8$$

where X, I are atomic number densities of Xe and I, respectively,

$\phi(r,t)$ is the time and space dependent flux,

λ_x, λ_i are the decay constants of Xe and I,

$\sigma_{a,x}$ is the microscopic absorption cross section of Xe,

Σ_f is the macroscopic fission cross section of fuel, and

Γ_x, Γ_i are the production yields of Xe and I.

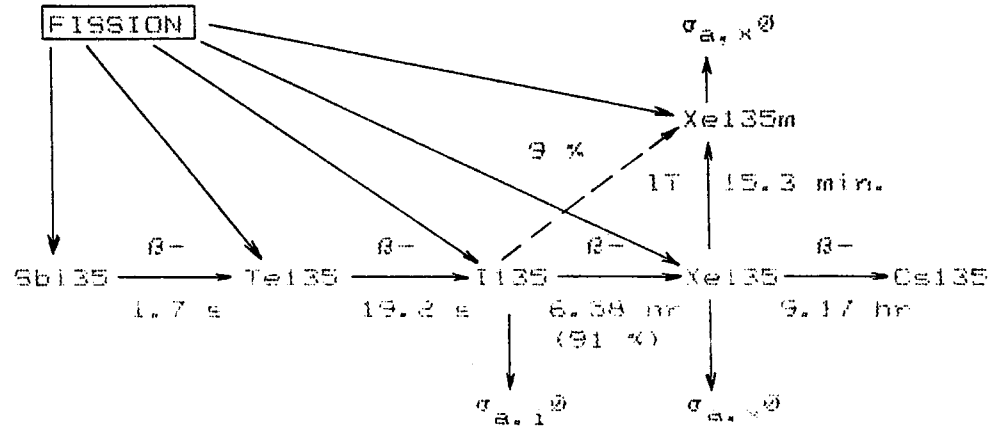


Figure 2.11 Production and removal of Xe-135 in fission

First two terms of Eqn 2.8 are the production rates of Xe-135 directly from fission and iodine decay, respectively. Last two terms represent the depletion rates due to decay and disappearance due to absorption.

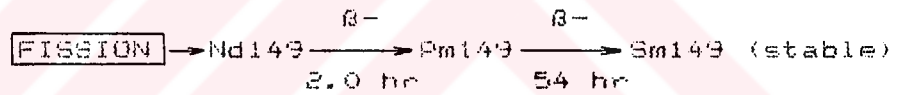


Figure 2.12 Production and removal of Sm-149 in fission

Similar analysis can be made for Sm-149 scheme which is given in Fig 2.12. But, in this case, Sm concentration must be evaluated from the following two equations:

$$\frac{\delta P}{\delta t} = \Gamma_D \Sigma_f \phi(n, t) - \lambda_D P(n, t) \quad 2.9$$

$$\frac{\delta S}{\delta t} = \lambda_D P(n, t) - \sigma_{a,S} \phi(n, t) S(n, t) \quad 2.10$$

where S, P are the time and space dependent atomic number densities of Sm-149 and Pm-149, respectively, $\Gamma_p \cdot \lambda_p$ are the fission yield and decay constant of Pm-149, and $\sigma_{a,s}$ is the microscopic absorption cross section of Sm-149.

Xe-135 and Sm-149 are especially important due to fission product poisoning. They show a high rate of increase at the start up and this period is called as the Xe and Sm transients. Here, significant amount of negative reactivity is spontaneously introduced into the system. Balancing of this reactivity was discussed in previous sections. After the transient state, each reaches an equilibrium value. By letting the time derivative of Eqn.s 2.8 to zero, equilibrium concentrations of Xe-135 (i.e. X_{eqm}), can be found as [3];

$$X_{eqm} = \frac{(\Gamma_x + \Gamma_i) \Sigma_f \phi(0)}{\lambda_x + \sigma_{a,x} \phi(0)} \quad 2.11$$

where $\phi(0)$ is the flux at time zero. Similarly, S_{eqm} can be written as [3],

$$S_{eqm} = \frac{\Gamma_s \Sigma_f}{\sigma_{a,s}} \quad 2.12$$

As seen from Eqn.s 2.11 and 2.12, equilibrium Xe-135 concentration is dependent on the initial flux, while the equilibrium Sm-149 concentration is independent of it.

Since the other fission products have small absorption cross sections (e.g. 29 barns for cesium, 25

barns for krypton, and 9 barns for lanthanum), they are lumped in one pseudo fission product in the fuel depletion analysis in LASER code.



CHAPTER 3

DEPLETION CALCULATIONS IN LASER

Since, the aim of the study is to find an optimal strategy for soluble poison utilization as control mechanism, and to investigate the effect of increase in enrichment on the core age, the change of reactor parameters with the boron injection into the moderator for certain fuel enrichments will be investigated in this research. The calculations are based on the depletion of fuel and of boron. The procedure that boron affects the core criticality was discussed before in detail. In this section, LASER, which is a cylindrical core, spatial and energy dependent depletion calculation program, will be shortly described.

3.1 A UNIT CELL BURNUP CODE LASER

3.1.1 Description of LASER

LASER is a multienergy, cylindrical unit cell burnup program written in FORTRAN IV based on the slowing down

code of MUFT and thermalization transport theory program of THERMOS [1,3,4,18].

An energy range of 0 to 10 MeV is considered in LASER with 1.855 eV cut-off energy between the fast and thermal energy ranges. Fast and epithermal energy range contains 50 different energy groups coinciding with that of THERMOS's. Thermal range has 35 groups of energy which coincide also with the MUFT's groups. The energy mesh of thermal region was such set up that the accurate representation of 0.3 eV Pu-239 resonance and 1.0 eV Pu-240 resonance were considered.

The code was restricted with one dimensional cylindrical geometry with reflected boundary conditions, and it carries out the depletion calculations for a unit cell (See Fig. 3.1) composed of 4 regions which are fuel, cladding, moderator, and an imaginary reflector. With this geometry, LASER allows linear or non-linear approach to space, time, and energy dependent solution of parameters for predetermined time steps. The number of space points that can be defined in the radial direction in the unit cell, is 14. Therefore, spatial depletion calculations of 7 isotopes of uranium and plutonium, xenon, samarium, and a lumped fission product in the fuel region, and the calculation of spatial distribution of flux over the entire cell are possible. In addition to 10 isotopes in the fuel region, hydrogen, deuterium, oxygen, aluminum,

zirconium, and steel can be considered in LASER as non-depleting materials used in cladding and moderator.

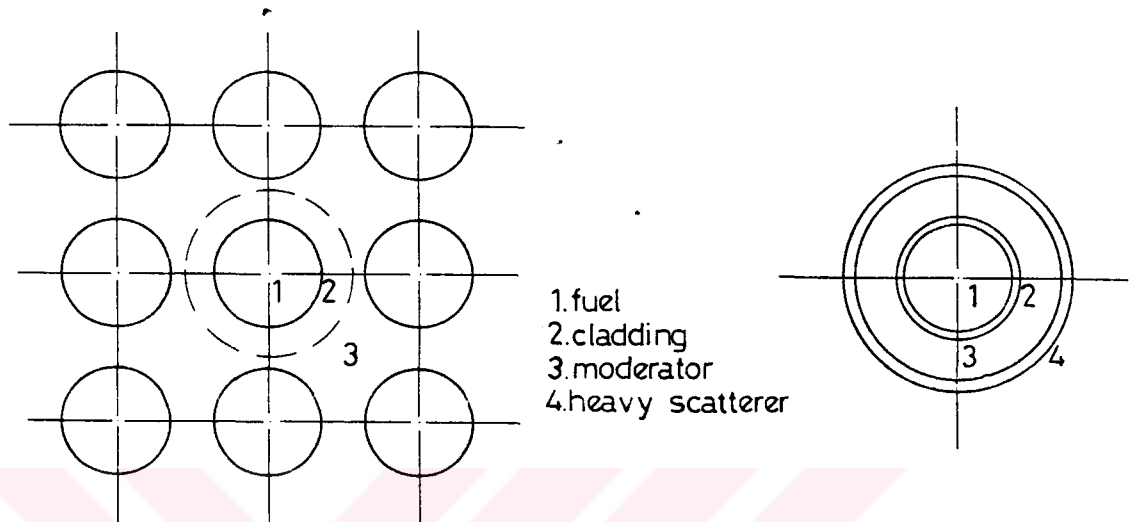


Figure 3.1 Unit cell of LASER for square batch

In moderator, water or heavy water can be defined with free gas scattering kernel and/or scattering Nelkin kernel [1,3], therefore, both PWR or HWR type reactors can be simulated in LASER. There are two pseudo materials in LASER those must be mentioned. One is the pseudo fission product in which all fission products except Xe-135 and Sm-149 are lumped, and the associated cross sections are calculated from polynomials as a function of burnup. Coefficients of polynomials are given in LASER input. The second one is the heavy scatterer used in the cell boundary for the reflecting boundary condition assumption. LASER assumes that the unit cell is identical over the entire core. This means the neutron current from a unit cell to the adjacent four, will be equal to the neutron

current from them to the unit cell. In other words, The net current through the boundaries of the unit cell is assumed to be zero. In this respect, for simplicity in calculations, an imaginary heavy scatterer is used at the boundary of the cell. Theoretically, for full scattering of neutrons, the thickness of the medium must be at least 2 to 3 mean free path of neutrons in that medium. Scattering cross section of the scatterer is given in LASER data, and the thickness of this imaginary reflector is kept the same in this study with the sample data.

3.1.2 Control Aspects of LASER

The main program of LASER has 28 subroutines, in which different links has been set up for different options. A flowchart for primary subroutines was given in App. B.

Seven data file definition is required in job control of LASER. Three of them are temporary files used for transferring data among the links. One of the permanent files is the thermal library file for MUFT calculations. The remaining ones are one input and two output files. Besides the ordinary output file which is printed out, a kind of input is generated for each time steps, or for predefined time steps which can be controlled in the program only. This output file is used as an input for continuing the problem which can be utilized in a great

extend due to system limitations. A list and simple descriptions of files are given in App. C.

3.1.3 Corrections and Additions

Although there are some corrections of LASER pointed out in its manual [1], some further ones were needed to run. Some variables other than the ones defined under the heading of two subroutines were required in convergence iteration of THERMOS calculations (See App. D). Besides, the initialization of one of the added variables to the heading, must be inserted into the same subroutines. Since the initial value of ROLD affects only the number of iteration, an estimation other than zero will be sufficient.

LASER performs the depletion calculations of U-235, U-236, U-238, Pu-239, Pu-240, Pu-241, Pu-242, Xe-135, and Sm-149 in subroutine NORM. For having the depletion of boron, some statements were added at the end of NORM. For any group of energy, the form of depletion equation is simply,

$$N(t) = N(0) \exp(-\sigma \phi t) \quad 3.1$$

This addition and some other related ones were given in App. D.

Boration of unit cell is provided by inserting a variable to the input of LASER in which the boron concentration in ppm unit must be given for each time

steps. Same addition was also provided on file 8. Related commands and formats can be seen in App. D.

3.2. INPUT OF LASER

The inputs of LASER were based on a sample PWR data given in Ref. 3, and the needed ones were tabulated below. Some of the input data of LASER remained the same, since they were general parameters. The parameters such as cell

Table 3.1 Sample PWR data

Thermal output	3411	MWt
Electrical output	1150	MWe
Efficiency	33.7	%
Fuel	UO ₂	
Coolant/moderator	H ₂ O	
Cladding material	Zircalloy	
Core		
Active height	366	cm
Equivalent active diameter	337	cm
Fuel loading	90200	kg
Fuel element array	17*17	
Number of fuel assembly/array	264	
Total number of fuel location	50952	
Fuel element pitch	1.25	cm
Fuel pellet diameter	0.819	cm
Cladding thickness	0.0572	cm
Average linear power density	178.0	W/cm

dimensions, number densities were calculated from the data given in Table 3.1. These calculations were based on the simple equations given in App. E. Xenon and samarium time steps were calculated from the time required for accumulation of equilibrium xenon and samarium concentrations. Solutions of Eqns 2.8 and 2.10 for xenon and samarium, will be discussed later in this section.

Table 3.2 Input of LASER for sample PWR ("+": estimated, "#": *E24 unit)

Buckling	0.2774 E-03	cm ²
Thickness of fuel region	0.4095	cm
Cladding thickness	0.0572	cm
Moderator thickness	0.23854	cm
Effective fuel temperature(+)	1473.0	K
Linear weight of fuel	0.48369 E-05	ton/cm
Linear power density	178.0	W/cm
Number density of water(#)	2.3476 E-01	mol/cm ³
Number density of zircalloy(#)	0.4225 E-01	atom/cm ³
Normal time steps(+)	5.184 E+06	sec.
Xenon time step	1.728 E+05	sec.
Samarium time step	1.1232 E+06	sec.

The last data those must be calculated, are the number densities of fuel isotopes and boron. Results of equations given in App. E for fuel composition at given enrichments used in this study, were tabulated below.

Boron concentrations will be given in ppm units on mass basis. Unit of ppm can be converted to number density by using the following relation,

$$N_b = N_{b, ppm} \frac{\mu_w N_o}{A_b} \quad 3.2$$

Table 3.3 Isotopic composition of UO₂ fuel for different enrichments (*E24 atom/cm³)

Enrich.	N _{U235}	N _{U238}	N _{O16}
2.1	.49806 E-03	.22926 E-01	.46848 E-01
3.2	.75894 E-03	.22668 E-01	.46854 E-01
4.0	.94866 E-03	.22480 E-01	.46858 E-01
4.8	.11384 E-02	.22293 E-01	.46862 E-01
5.6	.13281 E-02	.22105 E-01	.46867 E-01

where μ_w is the density of water, N_0 is the Avagadro's number, A_b is the atomic weight, and N is the number density. By substituting the numerical values as,

$$N_0 = 6.023 \text{ E}23 \text{ atom/mole.}$$

$$A_b = 10.81 \text{ amu, and}$$

$$\mu_w = 0.7017 \text{ gr/cm}^3 \text{ at } 300 \text{ }^\circ\text{C,}$$

one can find that;

$$N_b = N_b \cdot \text{ppm} * 3.909657 \text{ E-08} \quad 3.3$$

Control parameters for options were selected for the desired purposes in each run in the input of LASER.

3.2.1 Time Step Calculations

Burnup calculations are performed in LASER in the order of,

- i) initial time zero calculations,
- ii) xenon time step,
- iii) samarium time step, and
- iv) regular time steps.

Initial core parameters are evaluated at the initial time zero calculations of LASER. Then, Xe-135 and Sm-149 transients are considered with two successive time steps. Regular time steps start after these transient steps, and continue up to the given time.

The interval for the regular time step was selected as 2 months by considering that the frequent analysis will

give better results. Duration of xenon and samarium time steps can be calculated from the reduced cases of Eqn.s 2.8 and 2.10 due to LASER's limitations. For Xe-135, the equation will be as follows,

$$\frac{dX}{dt} = \Gamma_X \Sigma_f \phi - \lambda_X X - \sigma_{a,X} \phi X \quad 3.4$$

and for Sm-149, it will be,

$$\frac{dS}{dt} = \Gamma_S \Sigma_f \phi - \sigma_{a,S} \phi S \quad 3.5$$

Solutions of above equations were given in App. F. and results were tabulated at table 3.2.

3.2.2 Specific Power Calculations

As it was mentioned earlier, the core life can be discussed in different units but, usually MWD/T is used. Since the power production will increase with an increase in enrichment, some other unit describing both, burnup and fuel utilization was used in this study. This unit is the total power production per unit mass of spent fuel which is called specific power.

Hence, the total energy produced at the end of life (EOL) will be equal to,

$$E_t = \text{mass of fuel loaded} * \text{burnup} \quad 3.6$$

On the other hand, the total initial U-235 loading can be found by,

$$M_{U235} = \text{total fuel loaded} \frac{A_U}{A_{U02}} \% \text{ enrichment} \quad 3.7$$

Then, the mass of spent fuel will be,

$$\text{Spent U235} = \% \text{ depletion of U235} * M_{\text{U235}} \quad 3.8$$

Consequently, specific power P_{sp} , used in this research will be equal to,

$$P_{sp} = E_t / \text{Spent U235} \quad 3.9$$

in GWD/kg spent U-235 after the unit corrections.



CHAPTER 4

RESULTS

4.1 GENERAL

In three-zone fuelling, the enrichments used usually are 1.7, 2.1, 2.6, and 3.2 %. Since, boration can increase the core age by hardening spectrum, and producing more plutonium through the resonance absorption, the enrichments used in these calculations were taken as 2.1, 3.2, 4.0, 4.8, and 5.6 %. The drop in the fission rate of U-235 is compensated by the use of enriched fuel and higher rate of plutonium production.

If not otherwise stated, boration or deboration is done to keep the effective multiplication factor at 1.01, except the initial boration case. The effect of soluble burnable poison on the core parameters at different enrichments were investigated for the following cases;

- i) without boron,
- ii) boration only at the beginning,
- iii) periodic boration, and
- iv) periodic boration followed by periodic deboration.

In addition to these, the effects of initial boron concentrations, different boration strategies during the operation, and requirement to keep the k_{eff} at 1.03, were also investigated for 3.2 % enrichment. The criticality boron requirement of core at various enrichments of the fuel, was also carried out, and used as a comparison data.

The following abbreviations were used to shortly denote the several cases studied;

NB: No Boron,

IB: only Initial Boration,

PB: Periodic Boration,

BD: periodic Boration followed by periodic Deboration,

CB: Criticality Boron concentration,

BK: Boration plus deboration to Keep k_{eff} at 1.03,

DI: Different Initial boration, and

DB: Different Boration strategy for initial boration of case IB.

4.2. RESULTS OF BORATION STRATEGY SEARCH

General behaviours of the core loaded with 3.2 % enriched fuel is given in Fig 4.1, in terms of the k_{eff} and necessary theoretical boron concentration to keep the core critical. In Fig. 4.2, cell averaged thermal flux changes were plotted over the core life for the cases of NB, IB, and BD. Fast flux change of these cases were given.

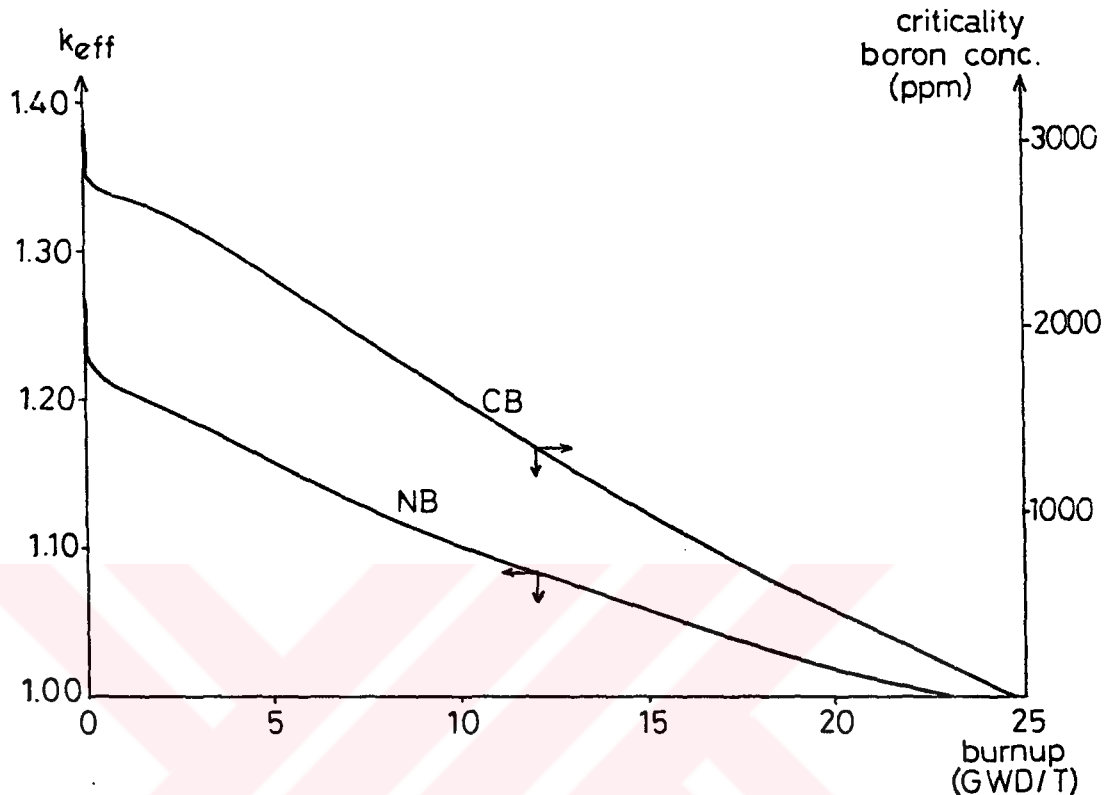


Figure 4.1 Change of k_{eff} and required criticality boron concentration for 3.2 % enrichment

seen in Fig 4.4. Effects of different amounts of initially used boron concentration on the radial thermal flux distribution in the unit cell was plotted in Fig 4.5 for the cases of NB, IB, and CB. The changes in k_{eff} at early stages of the core were given in Fig. 4.6 to show the effect of xenon transient state at 3.2 % enrichment. This is an enlarged scale view of Fig. 4.7 in which the overall changes of k_{eff} with burnup, for the same cases in Fig. 4.6 were plotted. The amounts of boron in ppm used in

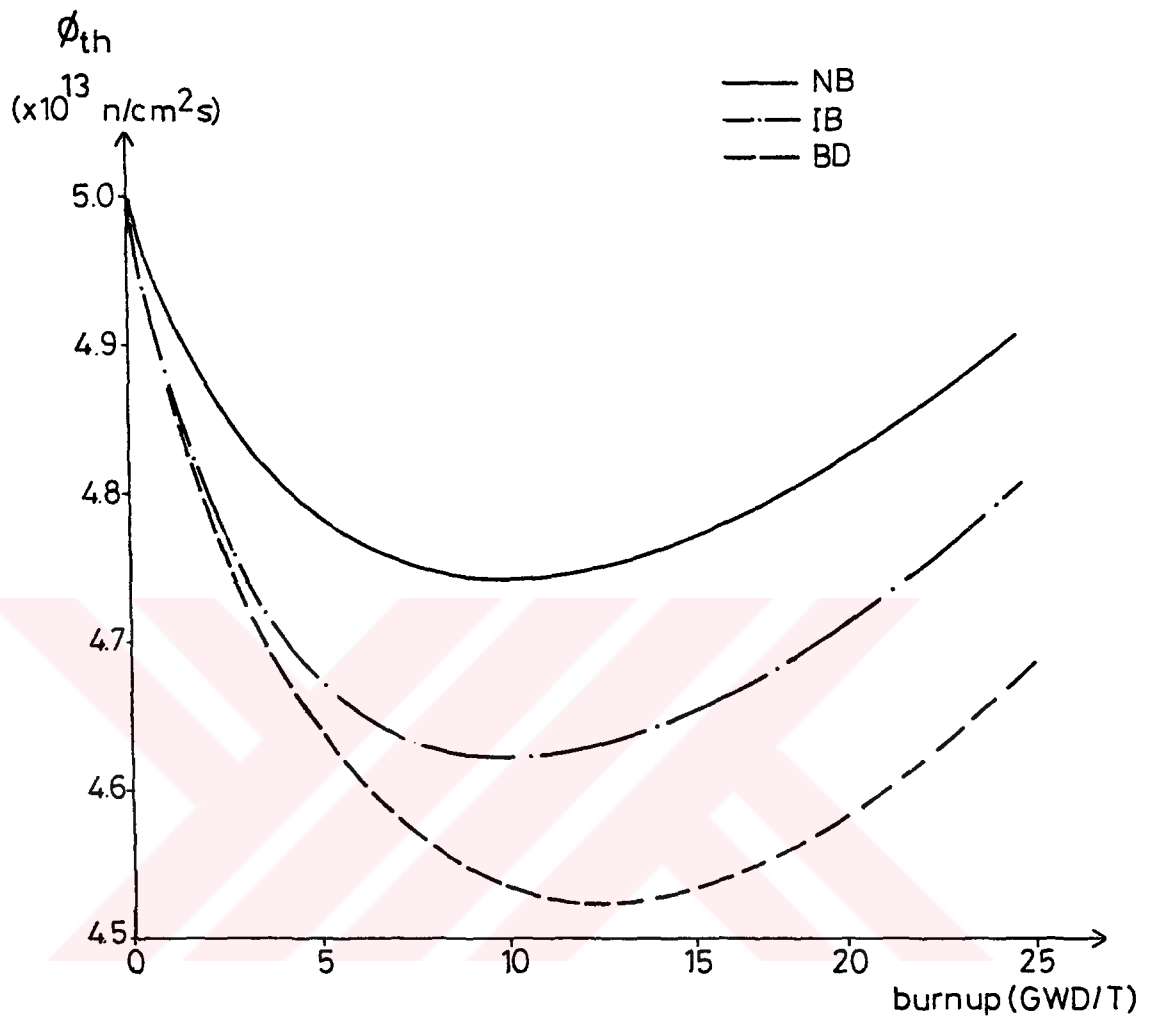


Figure 4.2 Cell averaged thermal flux

Table 4.1 Boron concentrations in ppm (percent values refer to the deboration amount)

T.S.	MWD/T	IB	PB	BD	CB	BK	DI	DE
initi.	-	2800	2800	2800	-	2700	2400	2800
Xe	74	-	-	-	2823	-	-	-
Sm	552	-	-	-	2726	-	-	-
1	2791	-	2380	2380	2546	2050	2200	2400
2	5029	-	2085	2085	2257	1750	1800	2000
3	7268	-	1775	1775	1950	1450	1300	1600
4	9507	-	1475	1475	1652	1150	-	1200
5	11746	-	1190	1190	1370	850	-	800
6	13984	-	920	920	1105	600	20 %	25 %
7	16223	-	665	665	850	400	40 %	50 %
8	18462	-	430	430	613	20 %	50 %	50 %
9	20700	-	-	50 %	388	40 %	30 %	30 %
10	22939	-	-	50 %	174	-	-	25 %

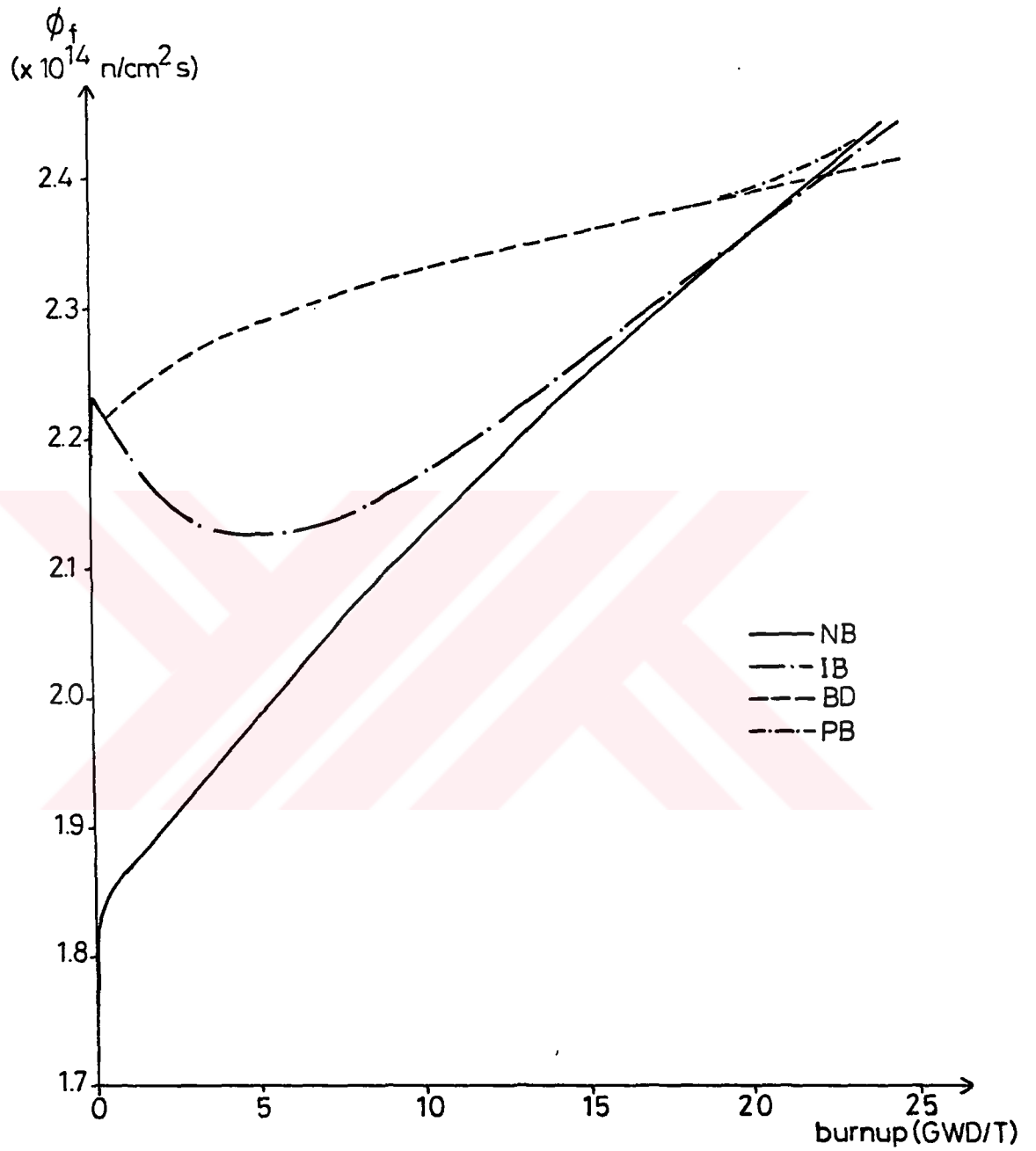


Figure 4.3 Cell averaged fast flux

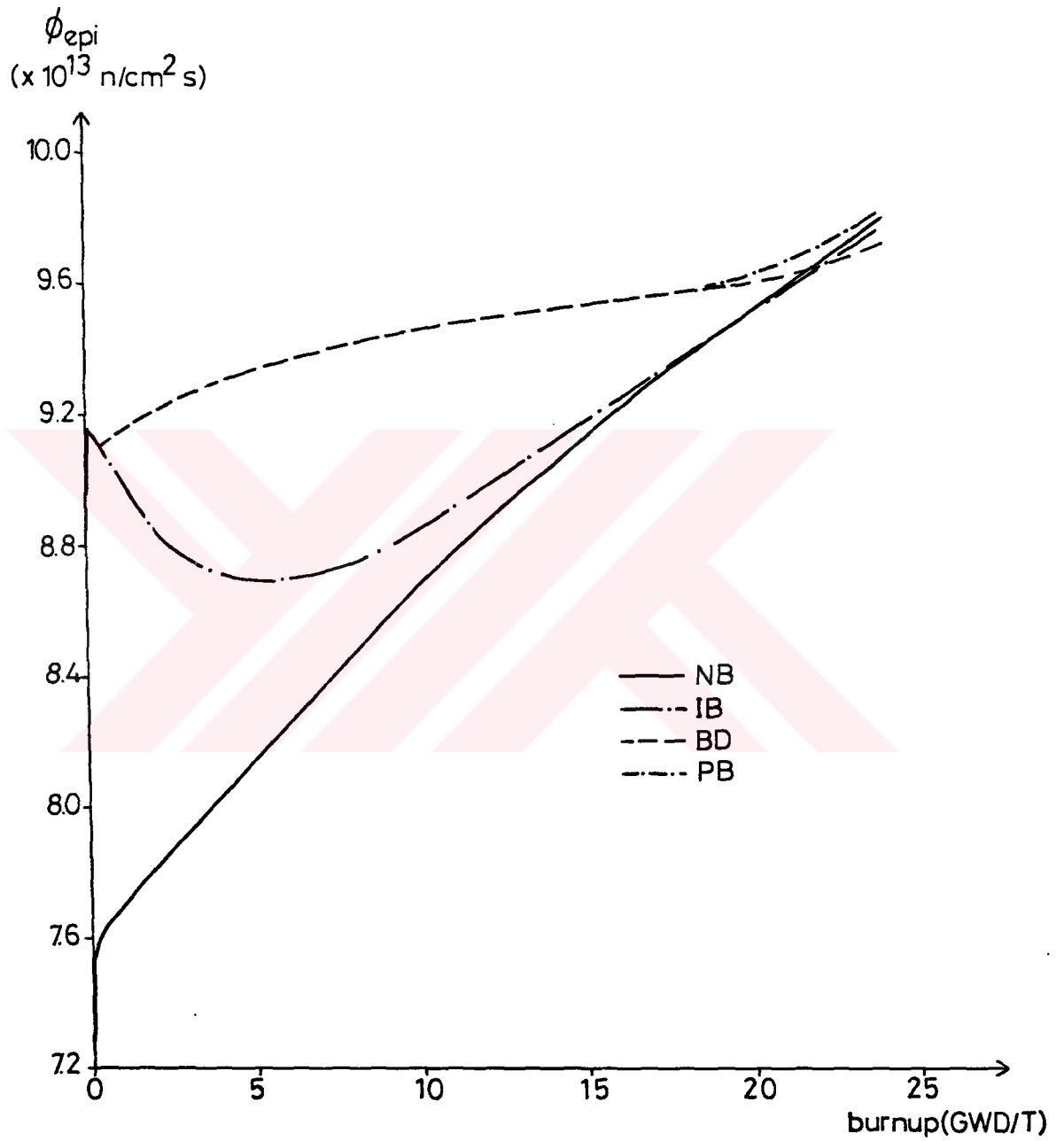


Figure 4.4 Cell averaged epithermal flux

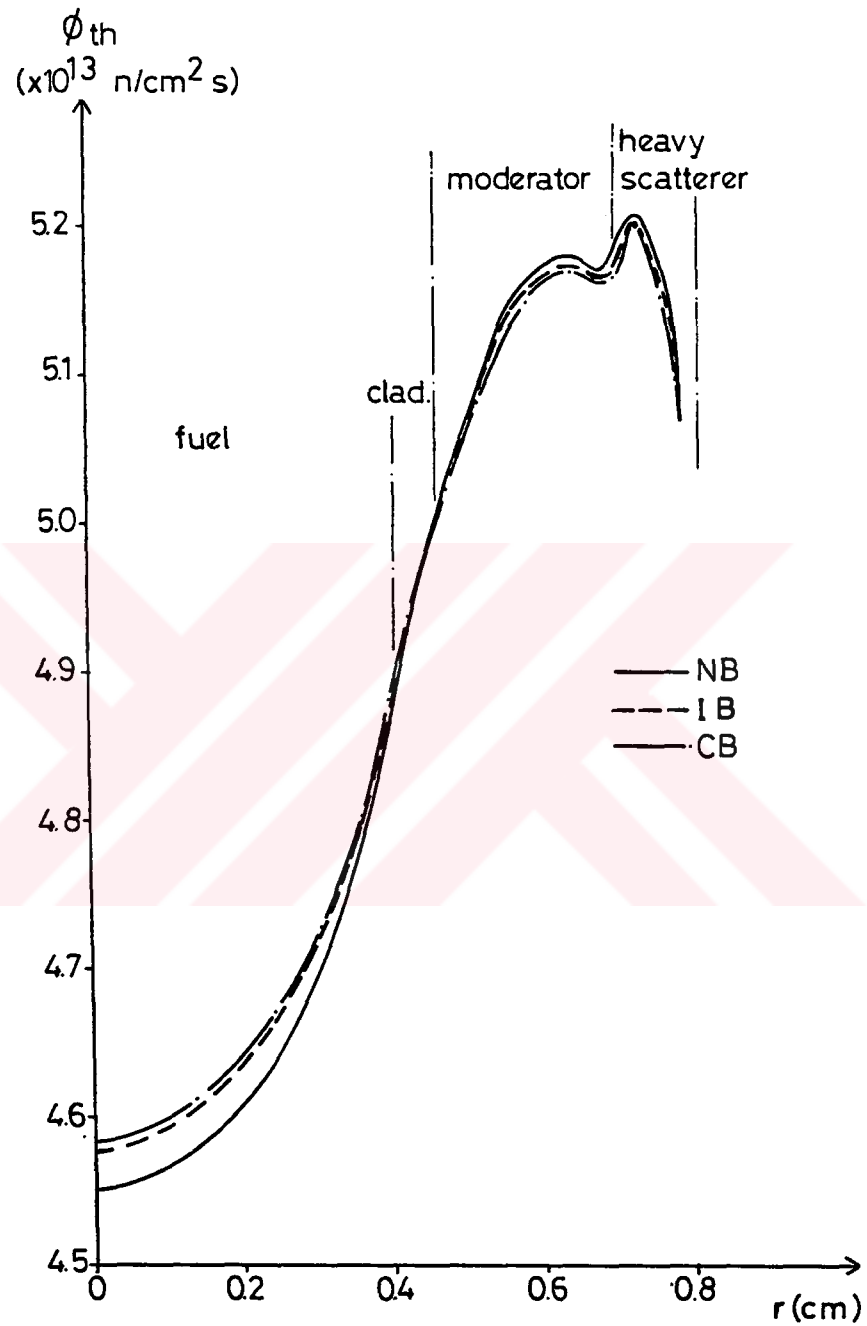


Figure 4.5 Radial thermal flux distribution for different initial boron values at the initial time step

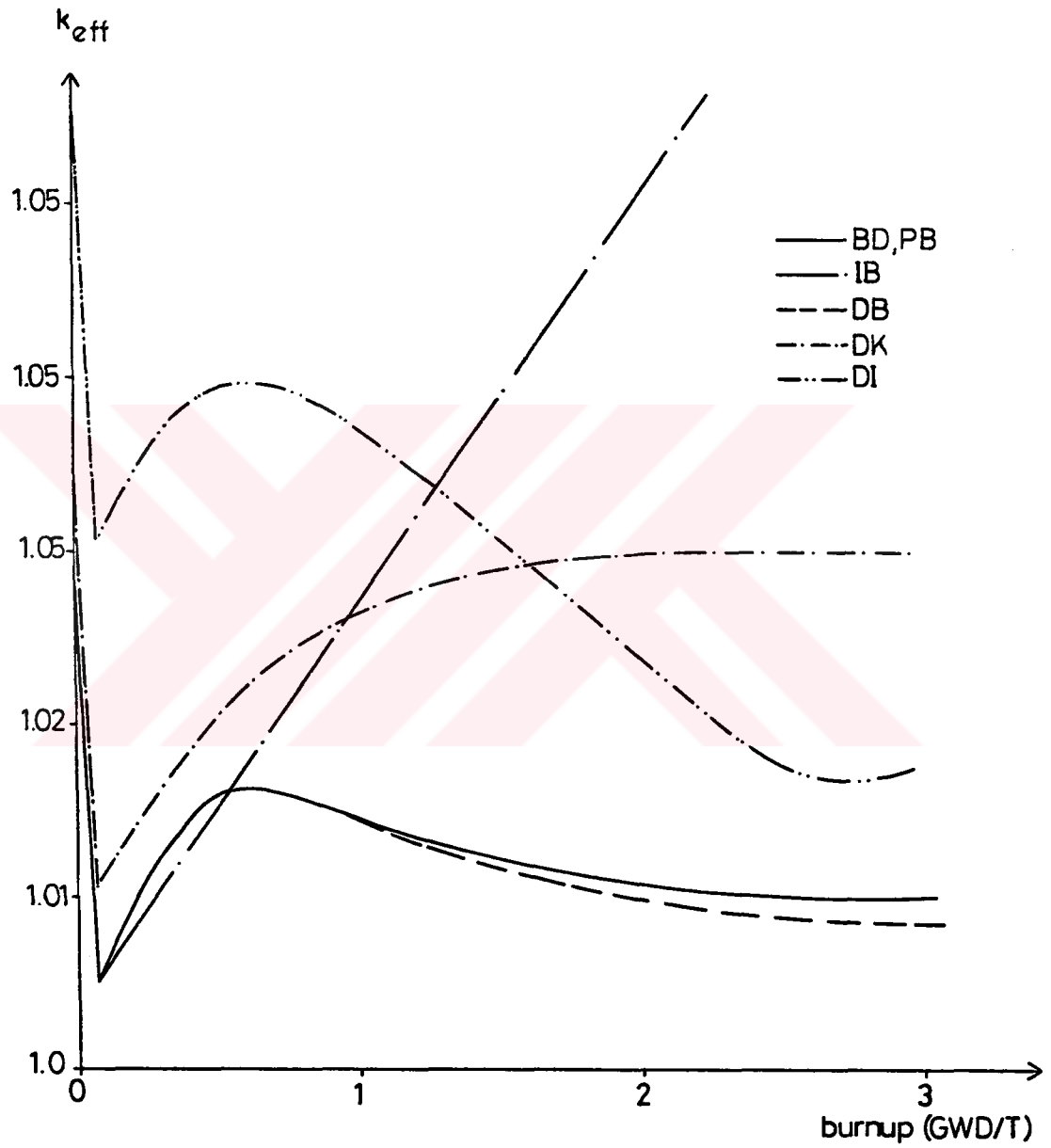


Figure 4.6 Xenon transients at early stages of core life

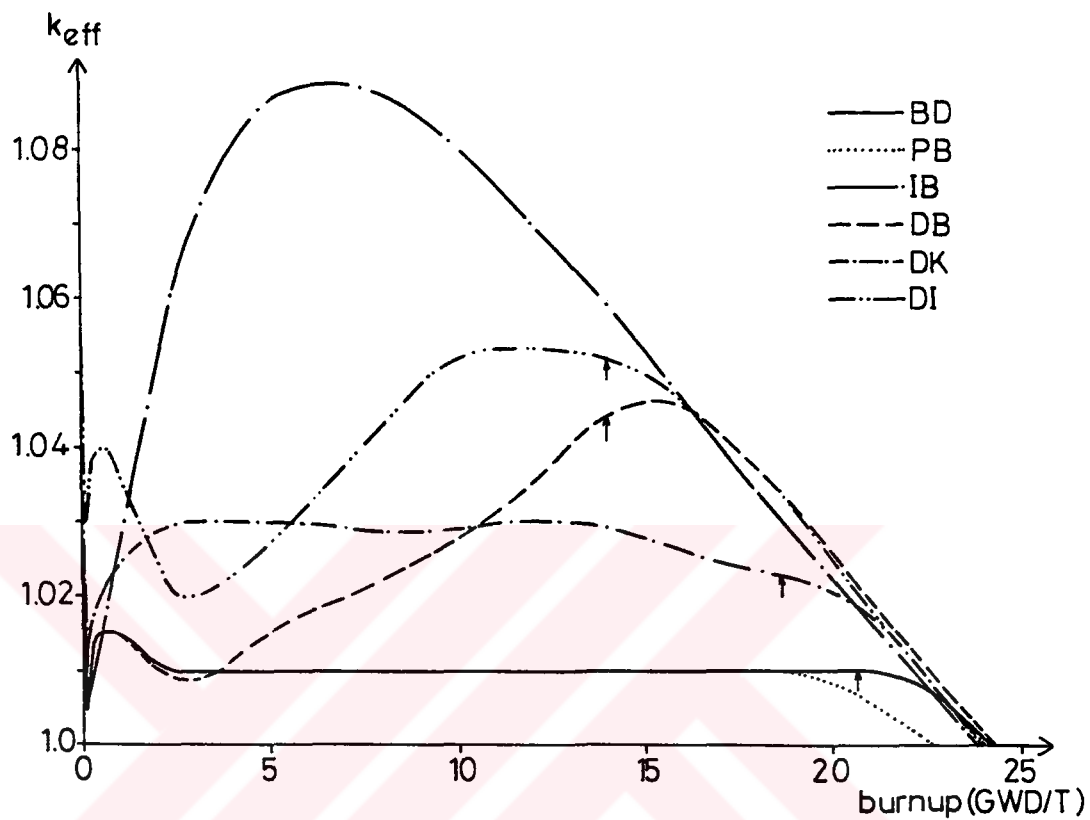


Figure 4.7 Changes of k_{eff} at different boration strategies for 3.2 % enrichment

LASER for different strategies were given in Table 4.1. The boron depletion was plotted for case CB in Fig. 4.8 as an example of depletion characteristic of boron, boration, and deboration. The main criterion for different strategies is the specific power, P_{sp} which is given in the last column of Table 4.2 together with other related parameters.

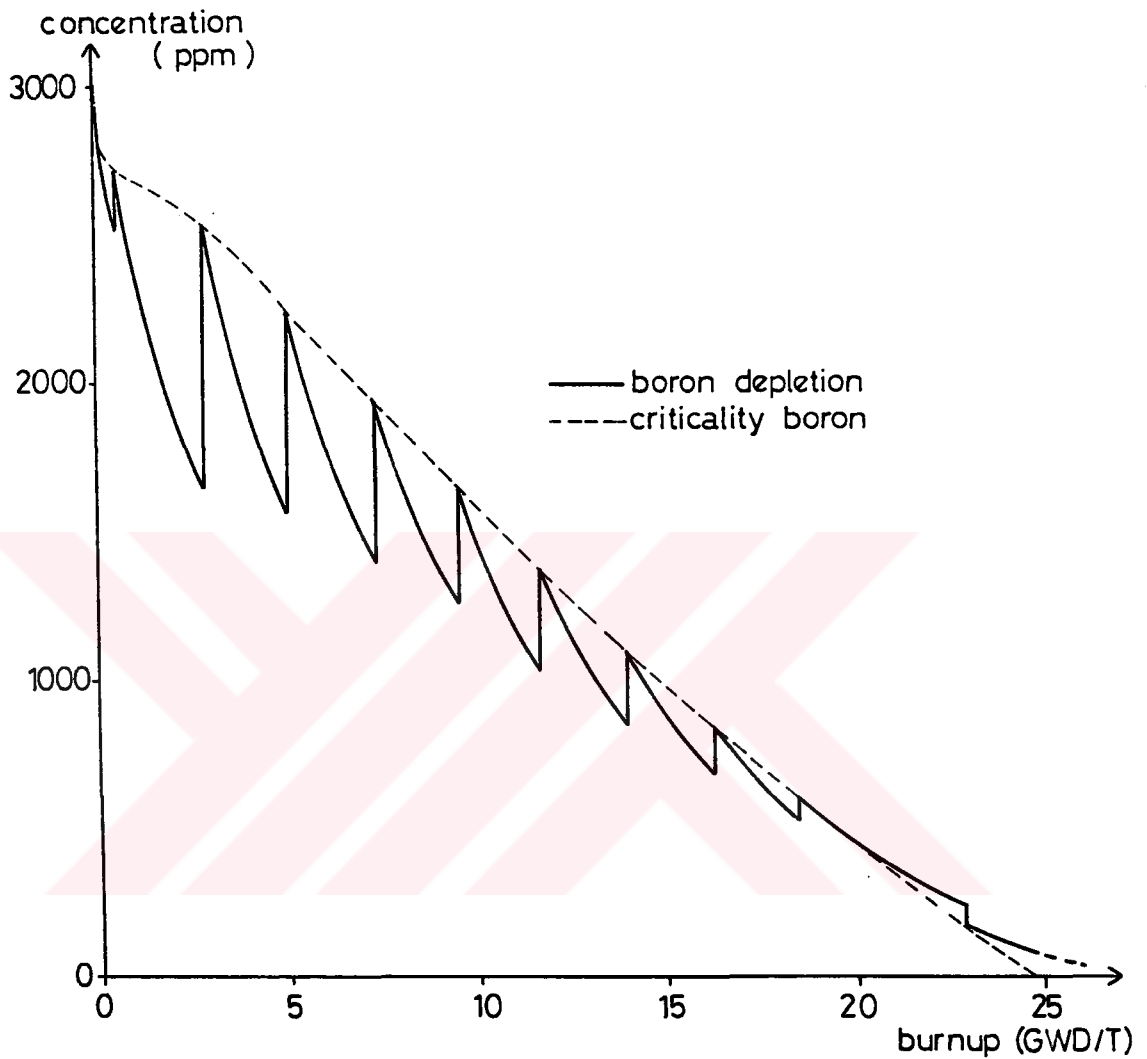


Figure 4.8 Depletion characteristics of boron in case CB

Table 4.2 Specific power calculations

Case	τ (GWD/T)	U235 depl. (%)	Spent U235 (kg)	P_{sp} (GWD/kg)
NB	23.34	57.177	1454.7	1.447
IB	23.73	56.922	1450.0	1.476
PB	21.76	53.069	1350.2	1.454
BD	24.00	56.670	1441.8	1.501
BK	24.02	56.928	1448.4	1.496
DI	24.03	57.226	1456.8	1.488
DB	24.21	57.334	1458.7	1.497

Additionally, EOL results of isotopic accumulations were given in Table 4.3.

Table 4.3 Some isotopic accumulated results at EOL

Case	Pu239 atom density	Energy production yields (%)			
		U235	U238	Pu239	Pu241
NB	1.3667 E20	61.653	7.417	27.656	3.205
IB	1.4111 E20	60.119	7.697	28.711	3.410
PB	1.4554 E20	60.831	8.016	28.033	3.050
BD	1.4621 E20	58.929	8.056	29.416	3.543
BK	1.4534 E20	59.248	7.915	29.237	3.524
DI	1.4338 E20	59.444	7.829	29.148	3.504
DB	1.4497 E20	58.999	7.909	29.446	3.569

4.3 RESULTS OF ENRICHMENT SEARCH

The changes of k_{eff} for different enrichments used in this research were given in Fig. 4.9. The necessary theoretical boron concentrations to absorb the excess reactivity were plotted in Fig. 4.10 for three of them.

The boron used at different enrichments to keep k_{eff} at 1.01 was tabulated in Table 4.4. The changes in k_{eff} by using these boron concentrations were plotted in Figs 4.11 through 4.14 for the enrichments 2.1, 4.0, 4.8, and 5.6 %, respectively. Cell averaged thermal flux of all enrichments were plotted in Fig. 4.15 during the burnup. EOL results of the cases IB, PB, and BD for new four

Table 4.4 Boron concentrations in each time step of BD cases in ppm units (% values refer to deboration)

T. S.	2.1%	3.2%	4.0%	4.8%	5.6%	TS	3.2%	4.0%	4.8%	5.6%
Ini.	1250	2800	4000	5130	6290	10	50 %	760	1565	2420
Xe	-	-	-	-	-	11	-	525	1300	2125
Sm	-	-	-	-	-	12	-	300	1040	1835
1	925	2330	3450	4555	5700	13	-	20 %	800	1565
2	675	2085	3150	4210	5325	14	-	40 %	560	1305
3	425	1775	2785	3830	4922	15	-	-	45 %	1055
4	185	1475	2450	3455	4517	16	-	-	50 %	812
5	28	1190	2130	3100	4125	17	-	-	50 %	573
6	-	920	1820	2770	3755	18	-	-	50 %	15 %
7	-	665	1535	2440	3390	19	-	-	-	50 %
8	-	430	1265	2135	3050	20	-	-	-	40 %
9	-	50 %	1000	1840	2730	21	-	-	-	-

enrichments were tabulated in Tables 4.5 through 4.8 in increasing order of enrichment. In addition, EOL accumulated fission product poisonings with the enrichment were plotted in Fig. 4.16.

Table 4.5 EOL results of 2.1 % enrichment

	τ GWD/T	U235 depl. %	energy yields (%)				Spent fuel kg	P_{sp} GWD/kg
			U235	U238	Pu239	Pu241		
IB	12.16	45.926	62.522	7.947	27.404	2.087	766.83	1.430
PB	11.33	43.488	63.396	8.105	26.586	1.875	726.12	1.407
BD	12.43	46.417	61.705	8.120	27.195	2.195	775.02	1.447

Table 4.6 EOL results of 4.0 % enrichment

	τ GWD/T	U235 depl. %	energy yields (%)				Spent fuel kg	P_{sp} GWD/kg
			U235	U238	Pu239	Pu241		
IB	31.27	60.466	60.216	7.563	28.275	3.853	1923.00	1.467
PB	30.21	58.313	59.725	7.949	28.491	2.743	1854.53	1.469
BD	31.68	60.181	58.775	7.956	29.156	4.013	1913.94	1.493

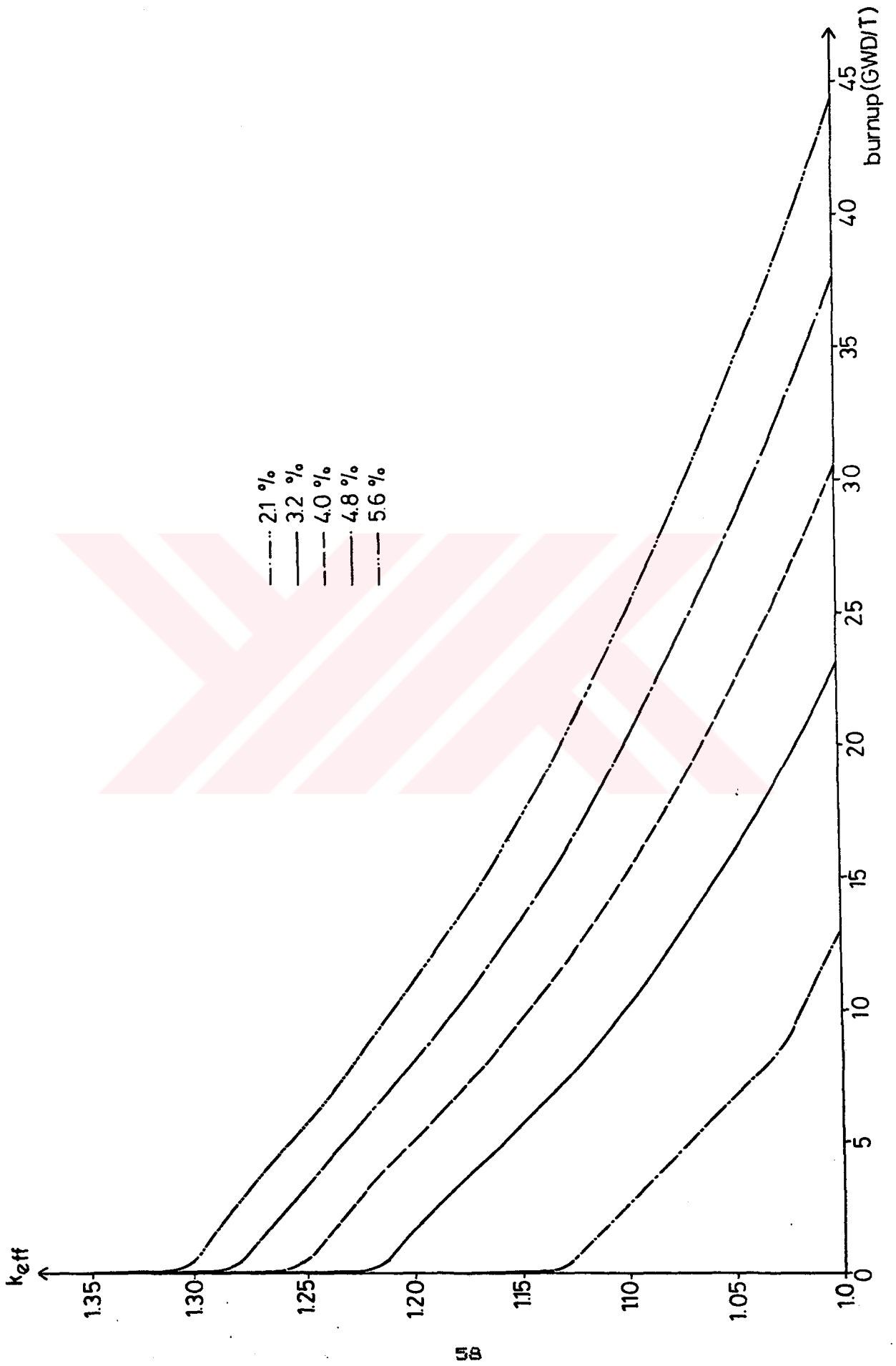


Figure 4.9 Changes of k_{eff} at different enrichments for NB case

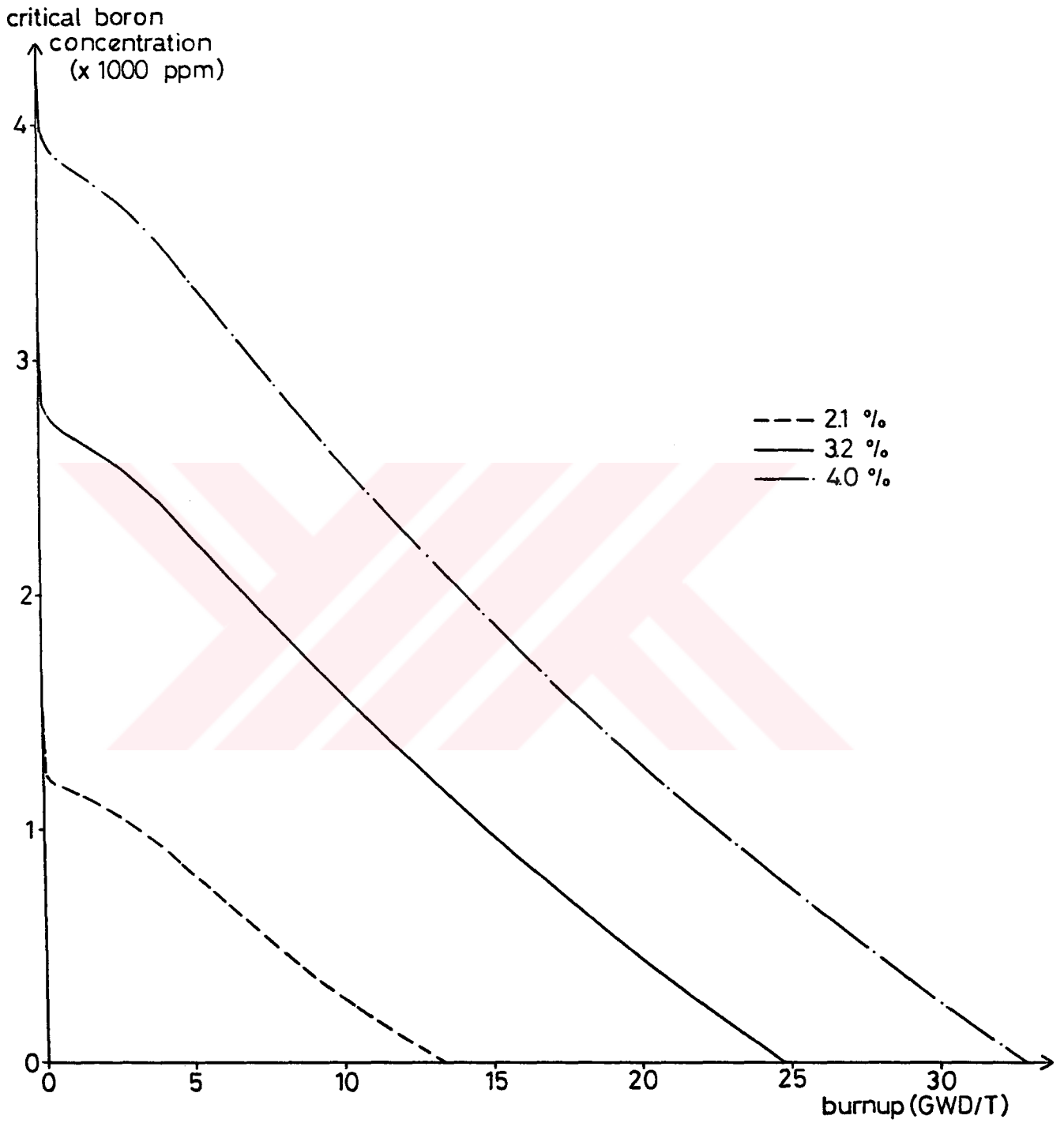


Figure 4.10 Criticality boron concentrations for CB case

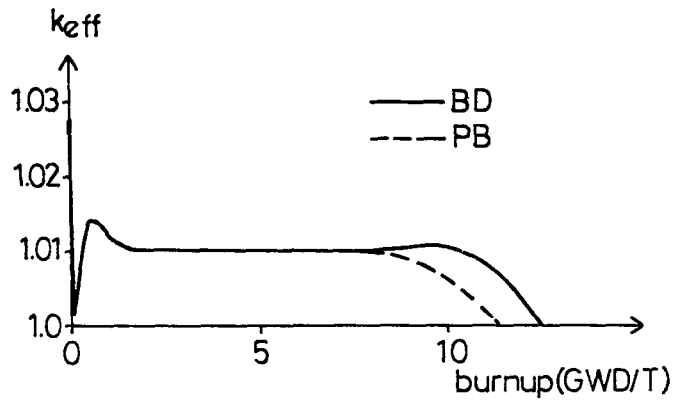


Figure 4.11 Change of k_{eff} for 2.1 % enrichment

Table 4.7 EOL results of 4.8 % enrichment

	τ GWD/T	U235 depl. %	energy yields (%)				Spent fuel kg	P_{sp} GWD/kg
			U235	U238	Pu239	Pu241		
IB	38.38	62.763	60.728	7.435	27.633	4.094	2395.22	1.445
PB	37.30	60.691	59.967	7.865	28.038	4.016	2316.15	1.453
BD	39.49	62.996	58.823	7.872	28.821	4.362	2404.12	1.482

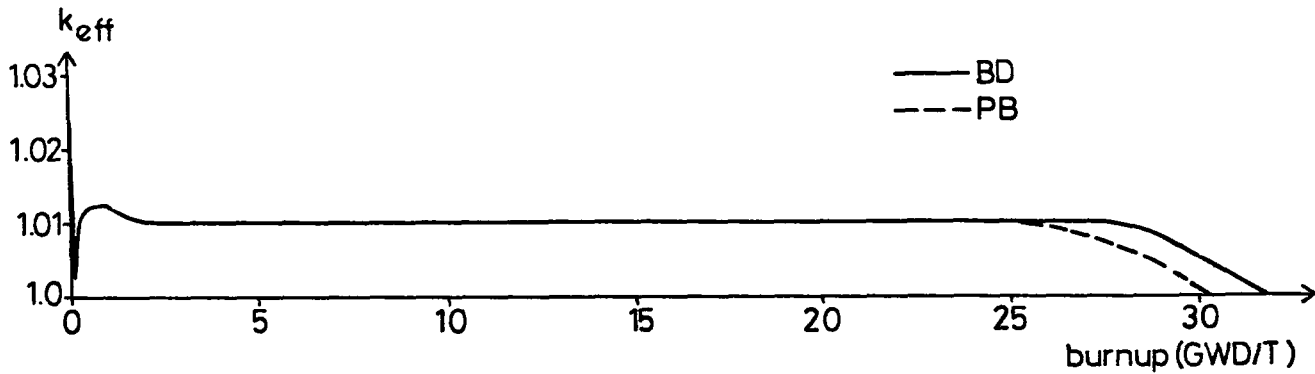


Figure 4.12 Change of k_{eff} for 4.0 % enrichment

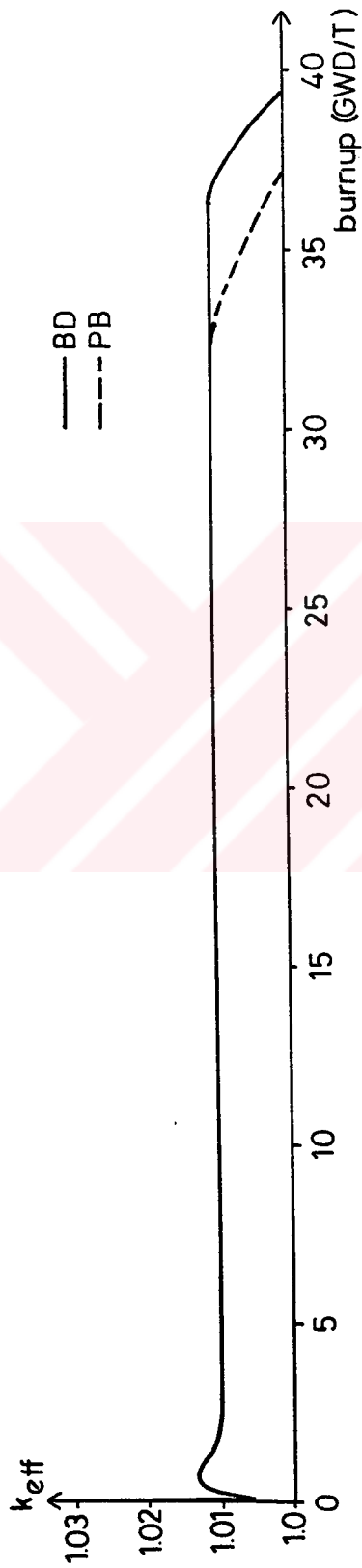


Figure 4.13 Change of k_{eff} for 4.8 % enrichment

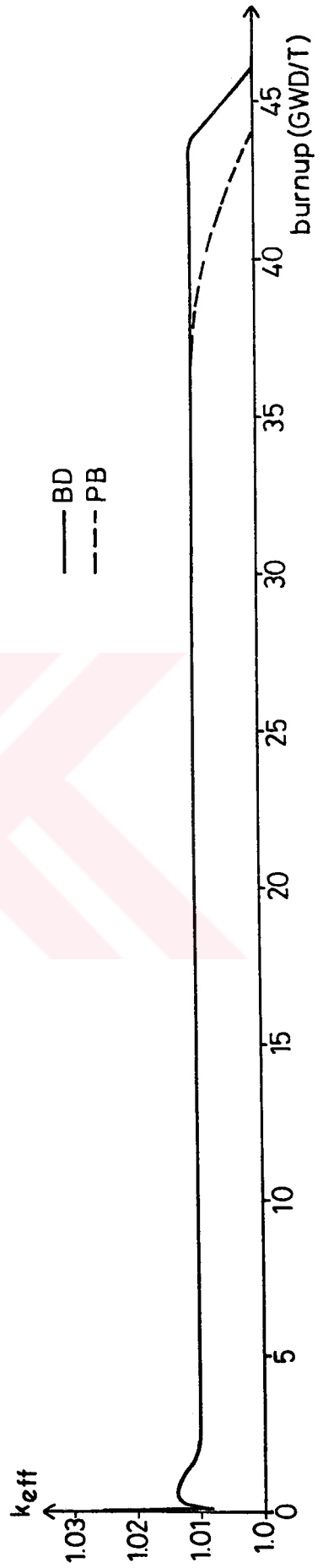


Figure 4.14 Change of k_{eff} for 5.6 % enrichment

Table 4.8 EOL results of 5.6 % enrichment

	τ GWD/T	U235	energy yields (%)				Spent	P_{sp} GWD/kg
		depl. %	U235	U238	Pu239	Pu241	fuel kg	
IB	45.21	64.448	61.346	7.322	26.971	4.232	2869.42	1.421
PB	43.97	62.271	60.469	7.782	27.457	4.158	2772.49	1.453
BD	46.41	64.511	59.580	7.788	28.194	4.362	2404.22	1.457

Finally, the results of specific power calculations were listed as a summary in Table 4.9, and they were plotted also in Fig. 4.17.

Table 4.9 Specific power calculations of cases BD at different enrichments

	2.1 %	3.2 %	4.0 %	4.8 %	5.6 %
τ (GWD/T)	12.41	24.00	31.68	39.49	46.41
Spent U235 (kg)	775.02	1441.80	1913.94	2404.12	2872.22
P_{sp} (GWD/kg)	1.447	1.501	1.493	1.482	1.457

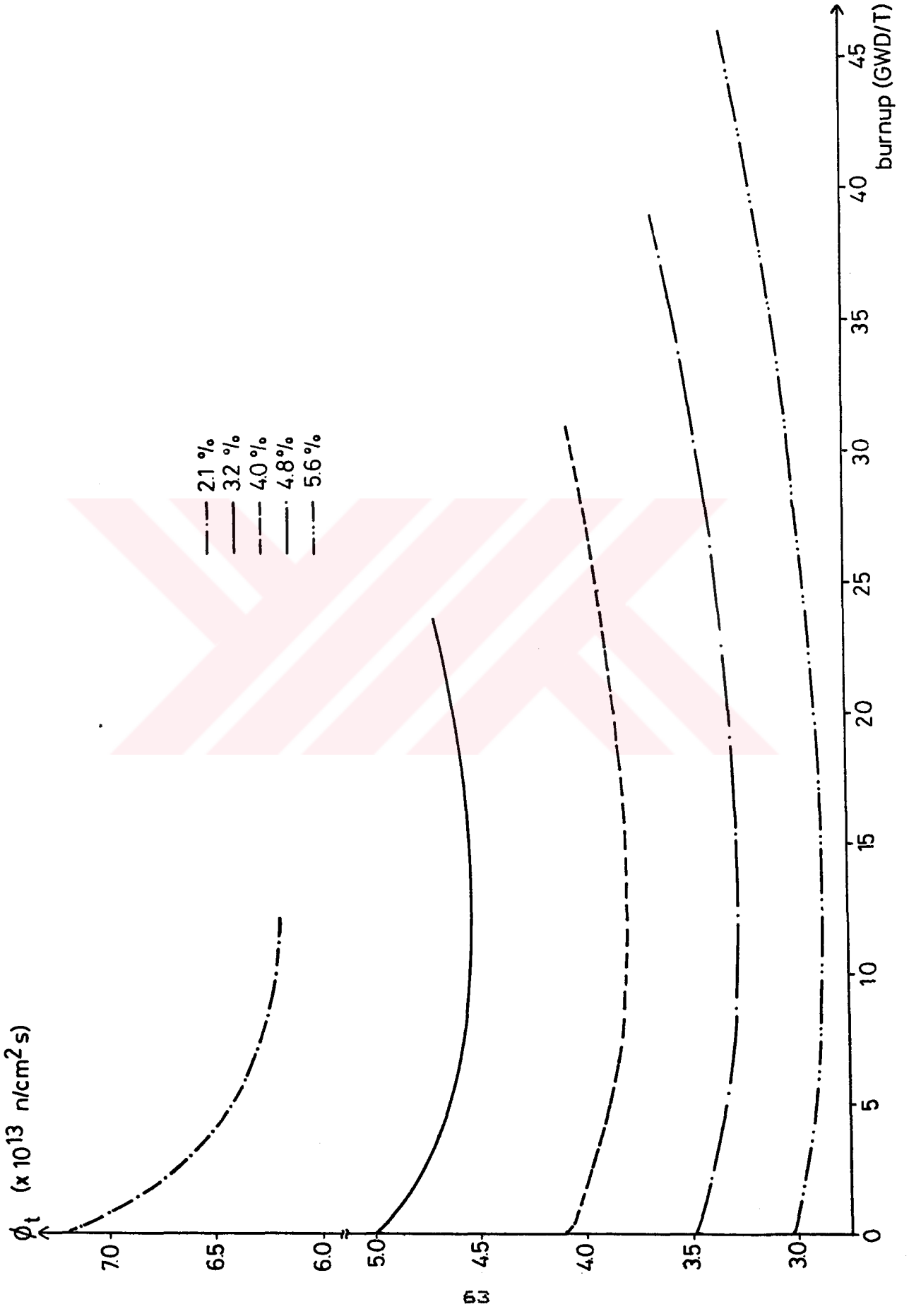


Figure 4.15 Cell averaged thermal flux change at various enrichments for BD case

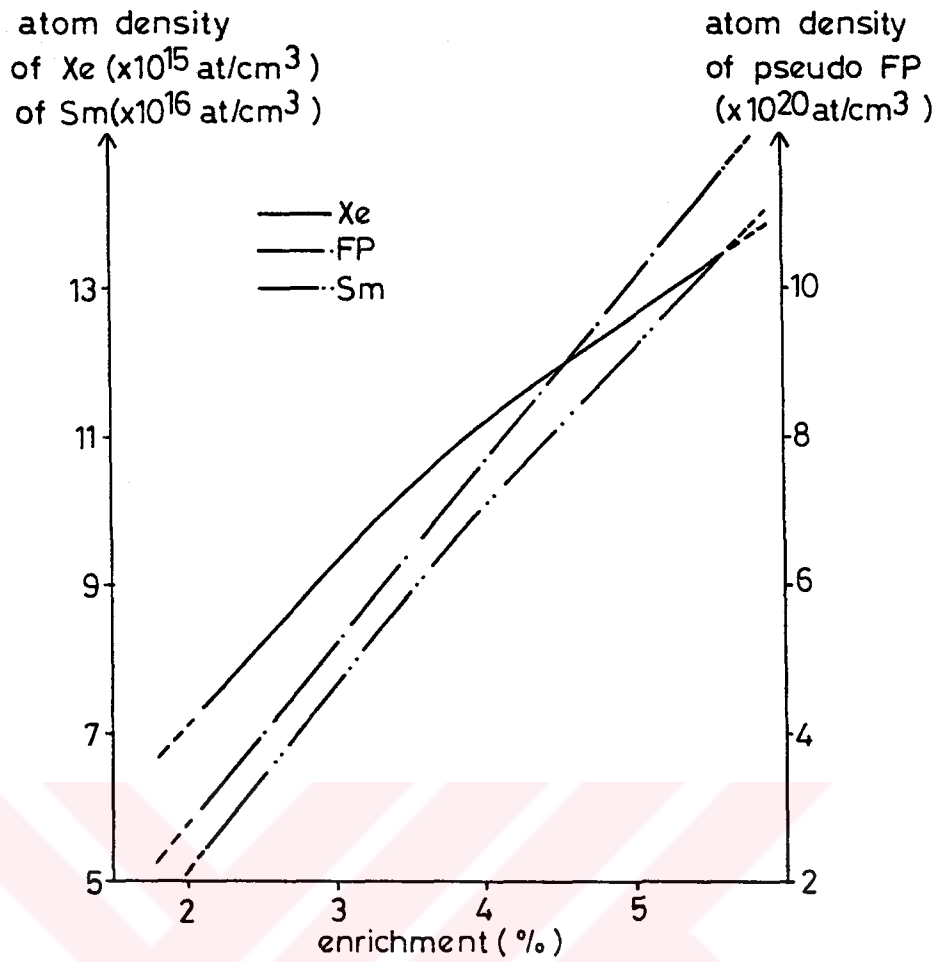


Figure 4.16 Fission product poisoning at EOL

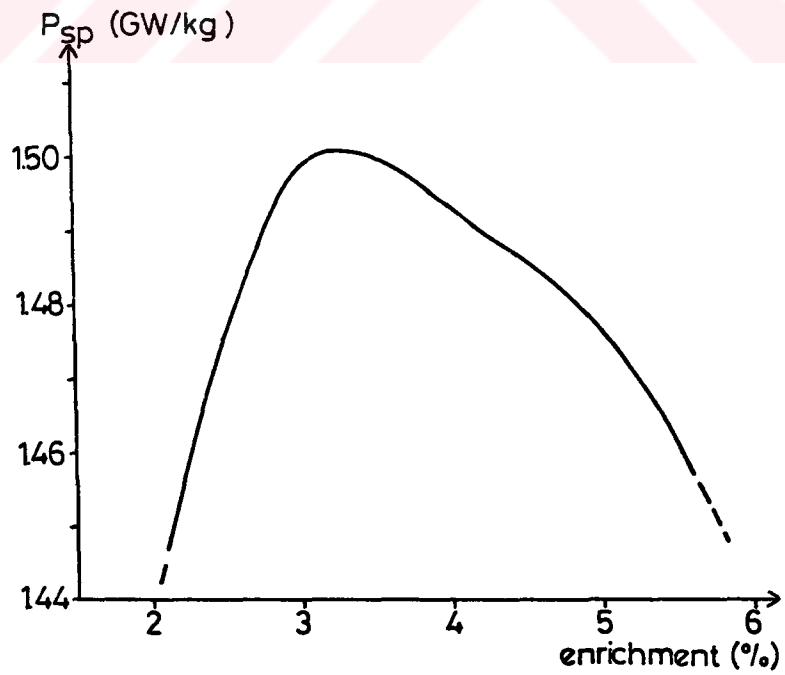


Figure 4.17 Change of specific power

CHAPTER 5

DISCUSSION

The main philosophy in decreasing the number of control rods in the core of a reactor, is to have more volume for fuel, and also produce more plutonium due to spectral hardening. In a nuclear reactor, the control of the excess reactivity is usually done by i) control rods and ii) fission product poisoning mainly by Xe-135 and Sm-149, which have exceptionally high thermal absorption cross sections. Control rods generally consist of isotopes which can be assumed to be non-depleting materials. Therefore, the number of control rods is directly proportional to the maximum excess reactivity that must be absorbed. If one can introduce a right amount of burnable poison into the core to absorb part of excess reactivity, then the necessary volume needed for control rods can be decreased. Although the past experience was to use fixed burnable poisons, preferably for xenon and samarium transient cycles, Galperin et al. [16] proposed the use of fixed burnable poisons in equilibrium cycles also.

In fact, the recent PWRs are designed to use the movable control rods only to overcome small transients and

to scram the reactor. The recent policy in in-core fuel management is to control the reactivity mainly by the fixed and/or the soluble burnable poisons, and to use control rods only to control a small fraction of the reactivity. Therefore, in this research, the control rods were assumed to control generally an excess reactivity of 0.01 at steady state operation, and to control the rest by soluble burnable poisons.

In a nuclear power reactor, a three-zone loading is usually done by using 1.7-2.1-3.2 % enrichments. Since the use of burnable poison necessitate higher fuel enrichments, 3.2 % was mostly used in the unit cell calculations in this research.

In the early stages of operation, the reactivity control is of primary importance, because there is no sufficient amount of Xe-135 build up, so the reactivity is at its maximum value. Therefore, the soluble poison requirement, i.e boron in LASER, is at its highest value.

With the use of boron in the moderator, spectral hardening and its effects come into sight in the core. Excess absorption of thermal neutrons causes depression of thermal flux, and hence, fast flux relatively increases, which is known as spectral hardening. Spectral hardening of flux distribution results in i) the decrease in U-235 depletion rate, ii) the increase in fast fission rate of U-238, and iii) the increase in Pu-239 production rate.

The last one also results in an increase in the production rates of further heavy isotopes of plutonium such as, Pu-241, and its fission rate. All these contribute to an increase in the core age.

In Fig. 4.1, the lower curve shows the change of k_{eff} with core age, and represents the amount of excess reactivity that must be controlled. The upper curve shows the theoretical amount of boron needed to keep the k_{eff} at 1.000 ± 0.0001 . At the very beginning, k_{eff} suddenly drops due to poison accumulation, i.e. xenon transient, and hence, necessary amount of theoretical boron concentration drops too. Then, k_{eff} and the boron requirement decrease gradually during the core life. At the EOL, core age is increased from 23.34 to 24.75 GWD/T by spectral hardening caused by boration, as it can be seen from burnup axis. This means 6 % gain in power.

Cell averaged thermal flux change over the core life can be seen in Fig. 4.2. It can be observed that, the flux shows the same behaviour whether boron is used or not. Thermal flux increases during the xenon transient stage to produce same power output against the Xe-135 accumulation in the very early part of the curves in Fig. 4.2. After the xenon transient is over, plutonium production by resonance absorption increases. Since the plutonium fission gives more neutron than does U-235, the flux must

decrease to keep the power constant as seen from the first part of curves in Fig. 4.2 for all cases. Besides Xe-135 and Sm-149, the lumped fission product of LASER also increases with burnup, and introduces further poisons into the core. When burnup reaches certain value, both effects balance each other. This is the minimum point in Fig. 4.2. After then, the negative effect of fission product build up overcomes the positive effect of plutonium production, and more flux is needed to keep power production constant. Then, the thermal flux starts to increase as seen from the second part of curves in Fig. 4.2. With the use of boron, thermal flux is depressed as expected, as seen from all three curves in this figure. It is noticed that, the minimum point of thermal flux shifts to the right as boron concentration increases. This should be due to the fact that as boron, and thus spectral hardening increases, less U-235 is consumed and more Pu-239 is produced. So, the fission rate of Pu-239 also increases. Since the fission of Pu-239 creates more neutrons than that of U-235, the negative effect of fission product build up can balance the positive effect of Pu-239 production at a later stage.

If boron is not used, fast flux gradually increases with fission product accumulation which also cause to spectral hardening as seen from Fig. 4.3. In xenon transient stage, the change in fast flux is very sharp. With the use of boron, initial fast flux increases from

about $1.76 \text{ E}14$ to $2.18 \text{ E}14$ neutrons/cm²s. If no further boron is used, fast flux decreases as seen from IB curve in Fig. 4.3 due to boron depletion, until it is balanced by fission product accumulation. After then, fast flux increases again as it is in NB case. But, further use of boron in successive burnups increases the fast flux as it is seen from BD curve. The epithermal neutron flux behaviours are also similar to fast flux as seen in Fig. 4.4 due to the same reason.

The effect of boron on initial flux distribution over the cell radius, is shown in Fig. 4.5. The thermal flux is depressed in the moderator region due to absorption by boron, whereas it is increased in fuel region to maintain the power constant as seen from the comparison of NB and CB curves.

The results of the use of boron on the xenon transient can be seen in Fig. 4.6 which is an enlarged plotting of early stages of Fig. 4.7. The k_{eff} shows a very sharp decrease due to combined effects of Xe-135 accumulation and the use of boron at the very early stages. Therefore, initial boron concentration is limited with the value of the k_{eff} at the Xe time step, i.e 0.074 GWD/T burnup. To keep the reactor still supercritical without control rods, initial boron concentration must not exceed a certain amount. If the initial boron concentration exceeds 2800 ppm for 3.2 % enriched fuel, k_{eff} may fall below 1.0 at the xenon time step.

If no more boron is used than the initially injected amount, k_{eff} shows a sharp increase due to the depletion of boron, and then, begins to decrease with the depletion of fissile materials in the fuel as seen in IB case in Fig. 4.6. The IB case results in 23.73 GWD/T age at the EOL. With the further boron utilization, the amount of excess reactivity that is assumed to be controlled by the control rods, can be decreased. The amount of boron used in each time step and deboration percentages used when necessary, were tabulated in Table 4.1 for all cases plotted in Fig. 4.6. In these cases, boron depletion calculations are based on the exponential equations as described in Chapter 3. Since the boron concentration can be controlled in LASER only at the beginning of each time step, the boron concentration shows a saw-tooth like behaviour as seen in Fig. 4.8, exponentially decreases between two time steps and jumps up at the beginning of each time step. In fact, boron depletion is so high at early stages of life that, its concentration will not be sufficient to keep the k_{eff} at desired level (e.g. 1.01), unless additional boron is injected into the moderator. The burnups in which deboration is started in each case, were pointed by an arrow in Fig. 4.7.

The use of boron in the first three time steps after the Xe and Sm ones, k_{eff} was depressed from the curve IB to the curve DB as seen in Fig. 4.7. In DB case, k_{eff}

gradually increases as in IB case, but at quite slower rate. Although deboration is started at about 14 GWD/T, k_{eff} keeps decreasing after 14 GWD/t due to the depletion of fuel also. In DB case, 24.21 GWD/T burnup is reached at the EOL which is 2 % more than that of IB case.

If a similar boration strategy is applied with the lower initial boration (i.e. 2400 ppm) as seen in curve DI, 24.03 GWD/T was reached which is obviously less than that of DB.

In the case of periodic boration, k_{eff} was decreased down to a constant level of 1.01 in cases PB and BD, and 24.00 GWD/T burnup was obtained by using deboration through the EOL in case of BD. PB is the case, in which highest amount of boron concentration were used in each time step. If the boron concentration is not controlled by also removal, the excess neutron absorption due to residual boron causes rapid shut down of reactor. In such a case (i.e. the case of PB), only 21.76 GWD/T core age was achieved, which is considerably smaller than the cases previously mentioned. The core age has been improved by deboration approximately 10 % in BD case over the PB case.

The behaviour of k_{eff} at 2700 ppm initial boron concentration, and different boration/deboration strategy to keep the k_{eff} at 1.03, i.e. BK case, was also given in

Fig. 4.7. Almost the same core age 24.02 GWD/T burnup was achieved in this case.

The main criterion that will be used in the comparison of all cases, is the specific power, which is defined earlier as power produced per unit mass of spent U-235, and the results of P_{sp} calculations were tabulated in Table 4.2. On this basis, BD with 1.501 GWD/kg spent U-235 showed the best fuel utilization among others. But, the BK and DB, with 1.496 and 1.497 GWD/kg respectively, have very close P_{sp} values to BD. In addition, DB achieved the highest burnup with 24.21 GWD/T which is 0.875 % more than that of BD. So, it seems that higher amounts of boron used in BD, causes a slight loss in neutron economy. Besides core age and specific power, one must also consider U-235 depletion, Pu-239 production, and volume occupied by control rods which is higher in DB, for a complete fuel strategy.

The control of BD is simpler than DB case due to steady characteristics of k_{eff} as seen in Fig. 4.7. In DB, there were continuous changes due to increasing and decreasing k_{eff} that must be simultaneously controlled by control rods. Although the DB has 0.875 % higher core age than that of BD, in P_{sp} basis, BD case has better fuel utilization due to low depletion percentage of U-235 at EOL. A qualitative comparison of all cases having close P_{sp} values, were given in Table 5.1.

Table 5.1 Case evaluation for various criteria

	better				worse
Control rod volume	Small	BD	BK	DB	Large
Pu239 production	High	BD	BK	DB	Low
U235 depletion	Less	BD	BK	DB	More
r core age	High	DB	BK	BD	Low
P_{sp} specific power	High	BD	DB	BK	Low

Consequently, the best boron utilization was found as the periodic boration-deboration strategy to keep the reactor at minimum excess reactivity for control rods, i.e. 0.01 in this study, for 3.2 % enrichment.

Four other enrichments were also studied in addition to 3.2 % . 2.1 % enrichment used in this research, was also a generally used enrichment in multi-zoned loading patterns of PWR's together with the 3.2 % . The other enrichments were selected arbitrarily by increasing the enrichments by 0.8 % in each case.

The amount of excess reactivity in each enrichments, can be seen in Fig. 4.9 in terms of the k_{eff} . All enrichments show the same characteristics, but the amount of excess reactivity increases with the fuel enrichment, which result in higher core age. More excess reactivity means more need for boron to keep the reactor at criticality as seen in Fig. 4.10. In all curves, Xe-135

accumulation behaviour was observed to be similar to 3.2 % enrichment as given in Fig. 4.6.

In Figs 4.11 through 4.14, k_{eff} behaviour of different enrichments for the case of BD were shown. It can be seen that the change in k_{eff} is almost similar except xenon transient. The magnitude of the decrease in k_{eff} at xenon transient, decreases with the increase in enrichment as seen in the very early stages of Figs 4.11 through 4.14. This is due to the decrease in thermal flux with the increase in enrichment (See Fig. 4.15). Xe-135 accumulation rate will decrease as the thermal flux decreases, which in turn, results in higher k_{eff} at xenon time step. This provides a flexibility in determination of initial boron concentration.

Since the macroscopic fission cross section of fuel increases with enrichment, the thermal flux must decrease to keep the power constant. The result of the use of boron is the flux depression, but as seen in Fig. 4.15, the ratio of the initial thermal flux to the minimum thermal flux, in other words the depression ratio decreases with enrichment. Since the flux decreases with enrichment, plutonium production rate will decrease due to lower flux. Then, fission product poison accumulation may tend to balance plutonium production at early stages. In fact, higher enrichments produce higher amounts of poisons as seen from Fig. 4.16. Therefore, the thermal flux tends to

increase by poison accumulation. Consequently, the minimum point results in a lower depression ratio in higher enrichments. But, since enrichment increases the core age, a rather smooth flux change is obtained at high enrichments as seen in Fig. 4.15. The minimum point is also shifted to the right at higher enrichments due to increased core age.

The Tables 4.5 through 4.8 show EOL isotopic, accumulated results for cases IB, PB, and BD for each enrichment. The BD case is better than IB and PB as far as U-235 depletion, and energy yields of fissile isotopes are concerned. In Table 4.9, a summary of specific powers, and core ages were tabulated. Since the higher core ages are expected due to highly enriched fuel loading, core age is not used as a comparison criterion. Also, atom density of Pu-239 produced, is such a parameter, increases with enrichment.

At 2.1 % enrichment, highest thermal flux results in highest fuel depletion rate. Besides, the initial loading of fissile isotope is so low that, it loses its critical mass in a very low EOL depletion percentage of U-235. Therefore, specific power of 2.1 % enrichment is found as 1.447 GWD/kg spent U-235, which is the lowest one among all enrichments. With the increase in enrichment, boron requirement, and thus spectral hardening increases. This leads to higher plutonium production rates, and to more fission. Therefore, fuel utilization can be improved by

increasing the enrichment. In 3.2 % enrichment, 1.501 GWD/kg spent U-235 specific power is achieved.

Further increase in enrichment results in the use of more boron, hence, further spectral hardening, and further plutonium production takes place. But, it also results in higher absorption rate of neutrons by boron, and increased production of fission products. As it is seen from lowest two curves in Fig. 4.15, further fission product poisoning causes higher thermal flux at EOL than the beginning thermal flux. This should be due to high amount of fission product and boron in the core.

The overall effect of enrichment on specific power can be seen in Fig. 4.17. The specific power shows a maximum at 3.2 % enrichment, lower and higher enrichments result in a decrease in the power obtained per kg of U-235 burnt.

Therefore, the use of boron at the maximum possible concentration to keep the k_{eff} at a low constant value (i.e. 1.01) in 3.2 % enrichment, gives better burnup, better fuel utilization, and better neutron economy compared to other enrichments, and boration strategies.

CHAPTER 6

CONCLUSIONS

1. Soluble poison can be used instead of control rods to absorb the excess reactivity in the core, when significantly large negative temperature coefficient is provided.

2. By using boron in moderator, the specific power of the core, U-235 depletion, Pu-239 production, and energy yields of fissile isotopes can be improved due to spectral hardening of neutron flux.

3. The minimum point of thermal flux change during the core life, is dependent on the amount of boron used, and shifts to the right on the burnup axis (i.e. more burnup) as boron concentration increases.

4. Deboronation improves the core life, and hence the specific power toward the end of life, when the depletion rate of boron decreased down to a limit.

5. Among different boration strategies, periodic boration followed by deboration toward the end of life, was found to be the best boration technique as far as core life and specific power are concerned.

6. Highly enriched fuel composition causes a decrease in the magnitude of the change in k_{eff} during the xenon transient step, meaning lower combined effects of boron and Xe-135 accumulation, and therefore, more initial boron concentration can be used. This causes further decrease in necessary control rods.

7. In high enrichments, high amounts of boron needed to keep k_{eff} at 1.01, and also high fission product poisoning result in poor neutron economy, and the best enrichment for optimum power production was found to be 3.2 %.

CHAPTER 7

RECOMMENDATIONS

The moderator temperature coefficient of reactivity is highly dependent on the boron concentration as it was mentioned in Chapter 2. The expulsion of moderator from the core by an increase in temperature, results in an expulsion of highly absorptive material from the core. Therefore, with the increase in boron concentration, α_T tends to be positive, unwillingly. Hence, it would be better to check α_T for boron concentrations used in the moderator. On the other hand, α_T is a function of temperature derivative of k as given in Eqn. 2.2. Since, the temperature of moderator is taken as constant in LASER, further improvement in LASER is needed.

The one dimensional analysis of the core, as it is in LASER, necessitates the single batch loading of the core. Since, the multi-zoned core loading patterns give better results in fuel management, LASER code can be modified for two dimensional analysis which allows the applications of advanced fuel management techniques. A similar work has been performed by Chang et al. [18], and LASER had been extended to two dimensional analysis.


Finally, it can be recommended that, the investigation of the effects of unit cell geometry on the core life, would be useful to find out the best geometry. In addition, since boration causes spectral hardening, the pitch distance optimization in a borated moderator is also recommended.



LIST OF REFERENCES

1. PONCELET, C.G., 1966, "LASER-A Depletion Program for Lattice Calculations Based on the MUFT and THERMOS", WCAP-6073, Westinghouse Electric Company.
2. LAMARSH, J.R., 1977, "Introduction to Nuclear Engineering", Addison-Wesley publishing Co., Reading, Massachusetts.
3. DUDERSTADT, J.J., HAMILTON, L.J., 1976, "Nuclear Reactor Analysis", John Wiley and Sons, Inc., New York.
4. LEVINE, S.H., 1981, "In-core Fuel Management Educational Module", Nuclear Technology, 53(June), pp.303.
5. POP-JORDANOV, J., 1973, "Advances in Local Nuclear Fuel Burnup Physics", Proceedings, Reactor Burnup Physics, pp.71, Vienna.
6. SILVENNOINEN, P., 1976, "Reactor Core Fuel Management" Pergamon Press, Oxford.
7. DOWNAR, T.J., KIM, Y.J., 1986, "A Reverse Depletion Method for PWR Core Reload Design", Nuclear Technology 73(April), pp.303.
8. HOBSON, G.H., TURINSKY, P.J., 1986, "Automatic Determination of PWR Core Loading Patterns That Maximize Beginning of Cycle Reactivity within Power Peaking and Burnup Constraints", Nuclear Technology, 74(July), pp.5
9. ANDREWS, M.G., MATZIE, R.A., SHAPIRO, N.L., 1985, "Cutting PWR Costs with Advanced In-core Fuel Management Techniques", Nuclear Engineering International, 23(Mar.), pp.34
10. AKE, T.N., McANDREW, R.G., WHITNEY, D.D., 1981, "Fuel Cycle Extension by Part Length Control Rod Removal at Rancho Seco", Nuclear Technology, 55(Dec.), pp.583
11. KODAH, Z.H., LEVINE, S.H., 1983, "Optimized Depletion of Lumped Burnable Poisons in PWRs", Nuclear Technology, 61(June), pp.487

12. GOLDSTEIN, L., STRASSER, A.A., 1983, " A Comparison of Gadolinia and Boron for Burnable Poison Application in PWRs", Nuclear Technology, 60(Mar.), pp.352
13. RADKOWSKY, A., CREAGAN, R.J., 1964, "Poison Control of Thermal Reactors", Proceedings, Third conference on the Peacefull Uses of Atomic Energy, UN, pp.277, Geneva
14. PERDIKIS, G.C., BAILEY, R.E., 1976, "A New Boron Control Law for Load-following PWRs", Trans. of American Nuclear Society, 23, pp.427
15. RONEN, Y., GALPERIN, A., 1983, "Modification of the PWR Control System Using a Gaseous Absorber", Annals of Nuclear Energy, 10(6), pp.331
16. GALPERIN, A., SEGEV, M., RADKOWSKY, A., 1986, "Substitution of the Soluble Boron Reactivity Control System of a PWR by Gadolinium Burnable Poisons", Nuclear Technology, 75(Nov.), pp.127
17. LLOYD, R.C., DURST, B.M., CLAYTON, E.D., 1979, "Effect of Soluble Neutron Absorbers on the Criticality of Low-Uranium-235-Enriched UO₂ Lattices", Nuclear Science and Engineering, 71, pp.164
18. CHANG, Y.Y., LOYALKA, S.K., 1981, "Reactor Fuel Burnup Calculation for a Square Lattice Cell", Nuclear Science and Engineering, 77, pp.235
19. "World Nuclear Industry Handbook 1987", 1987, Nuclear Engineering International



APPENDICES

APPENDIX A

NUCLEAR POWER CAPACITY PROJECTIONS

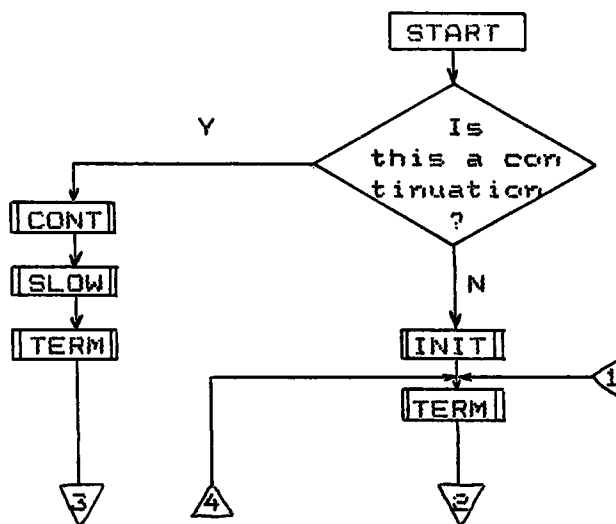
Table A.1 Nuclear power production (May 1985)

Countries	operable reactors		% of all elect.	capacity projections			
	unit	MWe		1990		2000	
				unit	MWe	unit	MWe
Belgium	8	5475	59.8	8	5475	9	6865
Canada	18	10981	12.7	21	13580	23	15342
Czechosl.	6	2380	14.6	10	3940	15	8392
France	45	39942	64.8	59	56997	69	70682
Germ. FR	19	16417	31.2	25	22982	25	22982
India	7	1265	2.2	10	1925	15	3025
Japan	34	23639	22.7	42	31758	58	47429
Spain	8	5577	24.0	10	7479	10	7479
Sweden	12	9605	42.3	12	9605	12	9605
Taiwan	6	4884	53.1	6	4884	8	6884
UK	38	11730	19.3	42	14220	43	15320
USA	100	85535	15.5	120	107555	124	112023
USSR	53	28005	10.3	103	70748	117	85766

APPENDIX B

CONTROL LAYOUT OF LASER

The subroutines seen in Fig. B.1 are the primary ones of LASER whose descriptions can be found in Ref. 1 in detail. Additionally, Fig. B.1 is a kind of simplified flowchart which is more straight forward but long in the main program due to the control capabilities. In simplification, control parameters except the MOR and MM, solution check control and counting parameters respectively, and some initialized parameters are kept out which make the different configurations necessary for each type of time step, such as initial, xenon, samarium, linear, and nonlinear time steps.



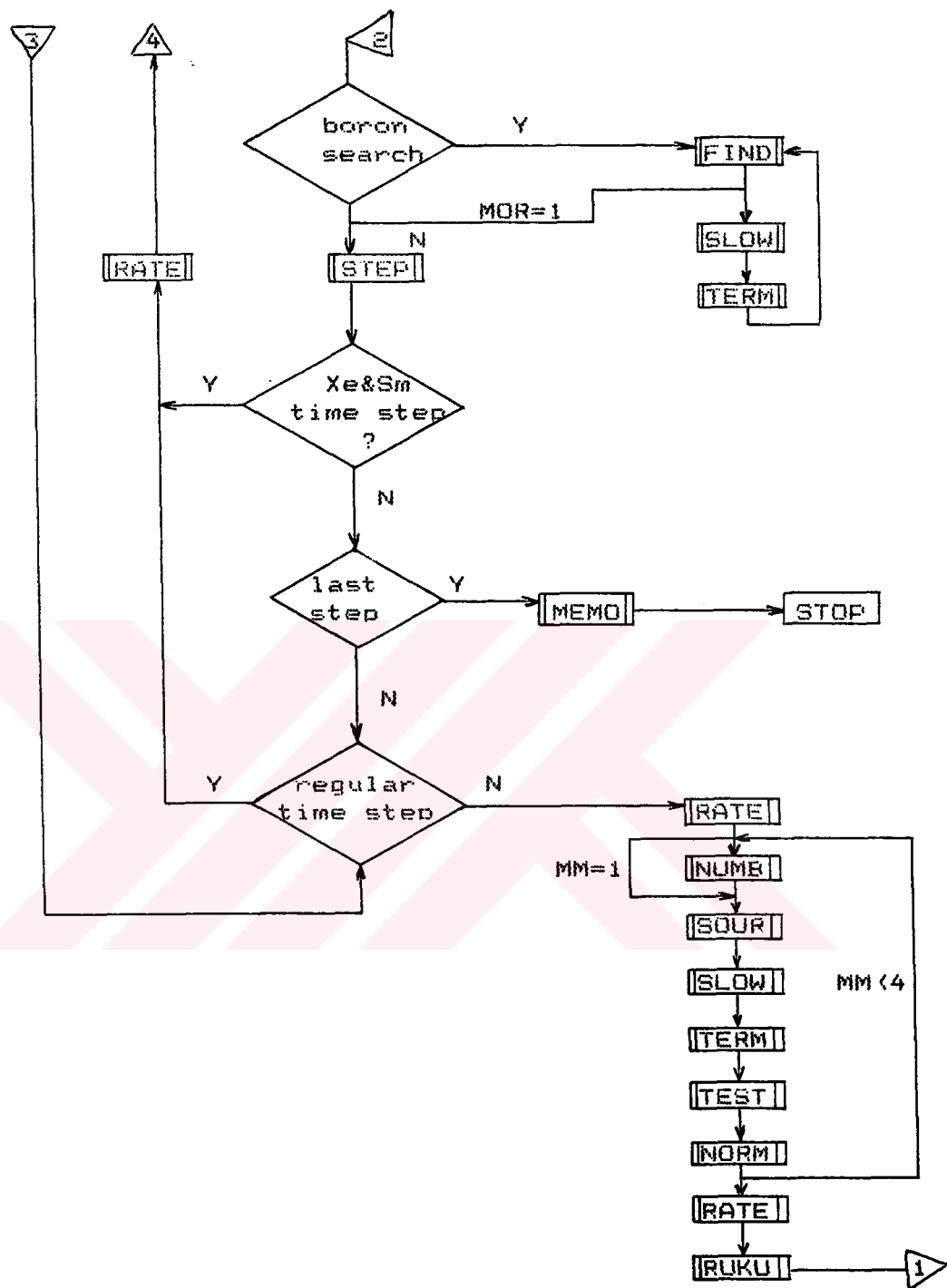


Figure B.1 General flowchart of LASER main program

APPENDIX C

FILES OF LASER

Table C.1 File descriptions that are used in LASER

No	file no	Descriptions
1	3	Temporary, THERMOS cross section and Kernel data
2	4	Temporary, MUFT and THERMOS results
3	10	Temporary, nonlinear burnup calculation results
4	5	LASER Input
5	6	LASER Output
6	8	Output for continuation problem
7	9	Thermal library

APPENDIX D

CHANGES IN LASER

1. Old heading,

```
SUBROUTINE RELAP(ITCNT,RNEW,OVER,EPS,ITMAX,RENORM)
```

must be changed to;

```
.....      .....      ...EPS,ITMAX,RENORM,ROLD,RELC,RELCA).
```

Same is true for SUBROUTINE RELAX and CALL commands of these two.

2. The new variables seen in the Fig. D.1 are,

RFABSB, rate of fast absorption of boron,

REABSB, rate of epithermal absorption of boron,

RTABSB, rate of thermal absorption of boron,

FERHAT, boron concentration in each time step, and

FERHAN, a dummy variable.

Rates are calculated by LASER but in some different variables, therefore, RFABSB, REABSB, and RTABSB must be equated related variables in subroutine STEP as;

```
      .  
      .  
      .  
133 .....  
      IF (I.NE.11) GO TO 135  
      RTABSB=RTABSB+SABTH(I,K)*VOLUME(K)  
135 CONTINUE  
140 CONTINUE  
      RTABSB=RTABSB/VOLMOD  
      .
```

```

      .
      .
      .
155 .....
      REABSE=SAB2(11)
      RFABSE=SAB1(11)
      .
      .

```

Also three of them must be initialized to zero at the beginning of subroutine STEP. In transferring of these new variables among the subroutines, the command of,

```
COMMON/RFABSE, REABSE, RTABSE, FERHAT(24)
```

must be inserted to the heading part of the main program, and subroutines INIT, STEP, NUMB, RUKU, MEMO, and CONT.

3. Since the writing to file 8 at MEMO, and reading from the same file at CONT are interrelated, formats must match each other, therefore it is not so important. But in

```

      IF(NONLI.EQ.1.AND.MM.NE.2.OR.SEARCH.EQ.2) GO TO 905
      ENC(15)=ENC(15)*EXP((-1)*(RFABSE+REABSE+RTABSE)*PILL*
#DT*XLAMDA(MM))
      X1BAR(11)=ENC(15)*VOLMOD/VOLC
      IF(FERHAT(NT).LE.0.0) GO TO 905
      IF(FERHAT(NT).GT.1.0) GO TO 930
      FERHAN=FERHAT(NT)*100.0
      WRITE(6,916) X1BAR(11),FERHAN
916 FORMAT(//,10X,"REAL BURNUP OF BORON: ",E10.5,///,10X,
#F4.1," % DEBORATION IS PERFORMED")
      ENC(15)=ENC(15)*(1.0-FERHAT(NT))
      GO TO 907
930 IF(XLAMDA(MM).NE.1.0) GO TO 905
      WRITE(6,915) X1BAR(11), FERHAT(NT)
915 FORMAT(//,10X,"REAL BURNUP OF BORON: ",E10.5,///,"NEW
#BORON CONCENTRATION IS: ",F6.1,"PPM",/)
      ENC(15)=FERHAT(NT)*3.903657E-08*0.198
907 X1BAR(11)=ENC(15)*VOLMOD/VOLC
905 CONTINUE

```

Figure D.1 Boron depletion calculations added to LASER

reading the initial parameters, F6.1 format was used. If the value that are read, is greater than 1.0, it means the boration in ppm units in reading amount. If it is between 0.0 and 1.0, it corresponds to percent deboration.



APPENDIX E

SOME BASIC EQUATIONS

Buckling of a cylindrical core is given as [2,3],

$$B^2 = \frac{2.405}{R} + \frac{\pi}{H} \quad \text{E.1}$$

where H and R are the active height, and equivalent active radius in cm, respectively, and are given in Table 3.2.

Equivalent radius of cell can be calculated for square lattice pitch from [2],

$$r = \text{pitch} / \sqrt{4} \quad \text{E.2}$$

and for 1.25 cm pitch, 0.819 cm fuel pellet diameter, and 0.0572 cm cladding thickness (Table 3.2), moderator thickness can be calculated from,

$$t_{\text{mod}} = r - t_{\text{fuel}} - t_{\text{clad}} \quad \text{E.3}$$

Linear fuel mass was calculated by knowing the 90200 kg initial fuel loading, 50952 fuel elements, and active height as follows,

$$\text{TON} = \frac{\text{tonne fuel loaded}}{\# \text{ of fuel element} * \text{active height}} \quad \text{E.4}$$

The number density of ordinary element is equal to,

$$N = \mu \frac{N_0}{A} \quad \text{E.5}$$

where N_0 is Avagadro's number,

ρ is the density of material, and

A is the atomic mass.

But, fuel number densities are dependent on the enrichment of the fuel, therefore, procedure will be as follows,

$$A_U = \frac{1}{\frac{\% \text{ U235}}{A_{\text{U235}}} + \frac{\% \text{ U238}}{A_{\text{U238}}}} \quad \text{E.6}$$

$$A_{\text{UO}_2} = A_U + 2A_O \quad \text{E.7}$$

Then, for the i th isotope of uranium in the fuel,

$$N_i = \%i \frac{N_0}{A_i} \frac{A_U}{A_{\text{UO}_2}} \mu_{\text{UO}_2} \quad \text{E.8}$$

and for oxygen,

$$N_O = 2 \frac{N_0}{A_{\text{UO}_2}} \mu_{\text{UO}_2} \quad \text{E.9}$$

can be used. The constants were taken from the literature as;

$$A_{\text{U235}} = 235.0439 \text{ gr/mole,}$$

$$A_{\text{U238}} = 238.0508 \text{ gr/mole,}$$

$$A_O = 15.9996 \text{ gr/mole, and}$$

$$\mu_{\text{UO}_2} = 10.5 \text{ gr/cm}^3$$

APPENDIX F

DETERMINATION OF XENON AND SAMARIUM TIME STEPS

Since the LASER considers only one pseudo fission product other than the Xe-135 and Sm-149, Eqn. 2.8 is reduced to Eqn. 3.4, and this equation can also be written in form of,

$$\frac{dX}{dt} + \lambda_X + \sigma_{a,X} \phi X = \Gamma_X \Sigma_f \phi \quad \text{F.1}$$

With the simple solution of first order differential equation (App. G) Xe-135 concentration depend on time can be found as,

$$X(t) = \frac{\lambda_X + \sigma_{a,X} \phi}{\Gamma_X \Sigma_f \phi} (1 - \exp(-(\lambda_X + \sigma_{a,X} \phi) t)) \quad \text{F.2}$$

Some tabulated values [2,3], and initial calculation results of LASER for 3.2 % enrichment were used in solution of Eqn. F.2. Then, for

$$\lambda_X = 2.09 \text{ E-05 s}^{-1},$$

$$\sigma_{a,X} = 2.7 \text{ E06 barns with } 0.8858 \text{ non-1/v factor,}$$

$$\Gamma_X = 0.064$$

$$\Sigma_f \phi = 0.36668 \text{ E13 fission/cm, and}$$

$$\phi = 0.31119 \text{ E14 n/cm}^2\text{s}$$

where last three were taken from LASER, it can be found that,

$$X(t) = 2.4618 \text{ E}15 (1 - \exp(-9.5326 \text{ E}-05t)) \quad \text{F.3}$$

When Eqn. F.3 is solved for 95 % equilibrium, time required was found as 31426 sec., i.e. about 9 hours. Then, it was assumed that, 2 days will be sufficient to achieve equilibrium for all enrichments. Therefore, xenon time step was chosen as 1.728 E05 sec. and tabulated in Table 3.3.

With similar reasons of xenon, Eqn. 2.10 is reduced to Eqn. 3.5 for Sm-149 and that can be written in form of,

$$\frac{dS}{dt} + \sigma_{a,s} \phi S = \Gamma_s \Sigma_f \phi \quad \text{F.4}$$

It was easily seen that, in LASER, Sm-149 is considered as a direct fission product against the actual case. Solution of Eqn. F.5 gives,

$$S(t) = \frac{\Gamma_s \Sigma_f \phi}{\sigma_{a,s} \phi} (1 - \exp(-\sigma_{a,s} \phi t)) \quad \text{F.4}$$

and with the additional data of,

$$\Gamma_s = 0.0113$$

$\sigma_{a,s} = 40800$ barns with 1.7568 non-1/v factor and solution can be written as;

$$S(t) = 1.8576 \text{ E}16 (1 - \exp(-2.2305 \text{ E}-06 * t)) \quad \text{F.6}$$

Duration for 95 % equilibrium accumulation was found as about 15 days. Then 15 days was chosen for all cases of this study as samarium time step. By considering the 2 days for xenon accumulation, 13 days, or equivalent of 1.1232 E06 seconds was used.

APPENDIX G

SOLUTION OF FIRST ORDER DIFFERENTIAL EQUATION

Consider a general form of equation is as follows;

$$\frac{dx}{dt} + ax = b \quad \text{G.1}$$

with the initial condition of $x(0)=0$. Eqn. G.1 can be modified as,

$$\frac{dx}{dt} = b - ax$$

$$dx = (b - ax)dt$$

$$dx = -a\left(x - \frac{b}{a}\right)dt$$

$$\frac{dx}{\left(x - \frac{b}{a}\right)} = -adt \quad \text{G.2}$$

By integrating two separated part, it can be found that,

$$\ln\left(x - \frac{b}{a}\right) = -at + c$$

$$\left(x - \frac{b}{a}\right) = \exp(-at) * \exp(c) = d * \exp(-at) \quad \text{G.3}$$

Now, the initial condition can be introduced to Eqn. G.3 and constant d can be found. At $t=0$,

$$\left(0 - \frac{b}{a}\right) = d * 1$$

Then,

$$d = - \frac{b}{a}$$

So, Eqn. G.3 can be rewritten as,

$$x - \frac{b}{a} = - \frac{b}{a} * \exp(-at)$$

$$x(t) = \frac{b}{a} - \frac{b}{a} \exp(-at)$$

In other words, the solution of Eqn. G.1 is equal to,

$$x(t) = \frac{b}{a} (1 - \exp(-at))$$

G.4

T. C.
Yükseköğretim Kurulu
Dokümantasyon Merkezi